Received: 29 March 2021 | Revised: 19 January 2022 | Accepted: 31 January 2022

DOI: 10.1002/hbm.25807

RESEARCH ARTICLE

WILEY

# Signatures of life course socioeconomic conditions in brain anatomy

Leyla Loued-Khenissi[1,2] | Olga Trofimova[1] | Peter Vollenweider[3] | Pedro Marques-Vidal[4] | Martin Preisig[4] | Antoine Lutti[1] | Matthias Kliegel[5] | Carmen Sandi[6] | Ferhat Kherif[1] | Silvia Stringhini[7,8] | Bogdan Draganski[1,9]

[1]Laboratory for Research in Neuroimaging, Department of Clinical Neuroscience, Lausanne University Hospital and University of Lausanne, Lausanne

[2]Theory of Pain Laboratory, University of Geneva, Geneva

[3]Department of medicine, Internal medicine, Lausanne University Hospital and University of Lausanne, Lausanne, Switzerland

[4]Department of Psychiatry, Lausanne University Hospital and University of Lausanne, Lausanne, Switzerland

[5]Laboratoire du Vieillissement Cognitif, Université de Genève, Geneva, Switzerland

[6]Laboratory of Behavioral Genetics, Ecole Polytechnique Federale de Lausanne (EPFL), Lausanne, Switzerland

[7]University Centre for General Medicine and Public Health (UNISANTE), Lausanne University, Lausanne, Switzerland

[8]Unit of Population Epidemiology, Primary Care Division, Geneva University Hospitals, Geneva, Switzerland

[9]Neurology Department, Max Planck Institute for Human Cognitive and Brain Sciences, Leipzig, Germany

**Correspondence**
Leyla Loued-Khenissi, Laboratory for Research in Neuroimaging, Department of Clinical Neuroscience, Lausanne University Hospital and University of Lausanne, Lausanne, Switzerland.
Email: lkhenissi@gmail.com

**Funding information**
European Commission, Grant/Award Number: 633666; Fondation Leenaards; Fondation Roger de Spoelberch; Louis-Jeantet Foundation; Schweizerischer Nationalfonds zur Förderung der Wissenschaftlichen Forschung, Grant/Award Numbers: 320030 184784, 32003B 135679, 32003B 159780, 3200B0 105993, 3200B0 118308, 33CS30 139468, 33CS30 14840, 33CSCO 122661

## Abstract

Socioeconomic status (SES) plays a significant role in health and disease. At the same time, early-life conditions affect neural function and structure, suggesting the brain may be a conduit for the biological embedding of SES. Here, we investigate the brain anatomy signatures of SES in a large-scale population cohort aged 45–85 years. We assess both gray matter morphometry and tissue properties indicative of myelin content. Higher life course SES is associated with increased volume in several brain regions, including postcentral and temporal gyri, cuneus, and cerebellum. We observe more widespread volume differences and higher myelin content in the sensorimotor network but lower myelin content in the temporal lobe associated with childhood SES. Crucially, childhood SES differences persisted in adult brains even after controlling for adult SES, highlighting the unique contribution of early-life conditions to brain anatomy, independent of later changes in SES. These findings inform on the biological underpinnings of social inequality, particularly as they pertain to early-life conditions.

**KEYWORDS**
multiparametric maps, quantitative MRI, socioeconomic status

Silvia Stringhini and Bogdan Draganski are last co-authors.

## 1 | INTRODUCTION

Low socioeconomic status (SES) contributes to negative health outcomes (Marmot & Bell, 2012), including cardiovascular disease (Kanjilal et al., 2006), diabetes (Stringhini et al., 2013), and decreased life expectancy (Stringhini et al., 2017). SES is further linked to differences in cognitive function (Aartsen et al., 2019). For instance, disadvantaged socioeconomic groups have an increased risk of dementia (Mayeda, Glymour, Quesenberry, & Whitmer, 2016), underscoring the putative link between brain health and SES (Resende, Guerra, & Miller, 2019). Evidence also points to a cumulative effect of socioeconomic disadvantage over time on health outcomes (Pollitt et al., 2008) highlighting the need to adopt a life course perspective when probing links between SES and physiological markers of health.

Links between SES and cognition support the notion that the brain is a plausible candidate for the biological embedding of SES, spurring several studies on the neural correlates of SES in the past decade. In the developing brain, childhood SES is tied to brain anatomy (Moriguchi & Shinohara, 2019) and function (Larsson, Solomon, & Kohn, 2015), such as reading abilities (Merz, Maskus, Melvin, He, & Noble, 2020). Specifically, hippocampal volumes correlate positively with SES (Hanson, Chandra, Wolfe, & Pollak, 2011); (Noble et al., 2015), as does cortical thickness (Lawson, Duda, Avants, Wu, & Farah, 2013). These observations suggest childhood SES may be associated with effects on language (Sarsour et al., 2011), reading abilities (Noble, Farah, & McCandliss, 2006), and mental health status (Reiss, 2013). Studies in adults are more limited, but generally support a link between SES and regional brain volumes (Elbejjani et al., 2017; Rzezak et al., 2015; Raizada & Kishiyama, 2010; Jednoróg et al., 2012), although a recent meta-analysis served to highlight the diversity of specific SES neural correlates across studies (Yaple & Yu, 2020).

Studies on the neural imprints of SES nevertheless remain comparatively sparse (McDermott et al., 2019) and at times yield varied results (Farah, 2017; Yaple & Yu, 2020). Further, studies have more often relied on region-of-interest (ROI) analyses rather than a whole-brain investigation (Farah, 2017; Yaple & Yu, 2020), leaving results open to bias (Poldrack, 2006). The tendency to limit analyses to specific regions may reflect the nature of the feature studied. SES presents a social construct, as opposed to a nosological entity, and therefore, corollary neural differences in the population should be subtle, requiring large-scale studies to be identified at the whole-brain level.

It further remains unclear whether SES-related differences in late-life reflect traces of childhood SES, as the latter may resolve with a higher SES in adulthood or maturation, or, conversely, persist into old age. A large body of literature has identified lingering effects of childhood deprivation on adult well-being (Duncan, Ziol-Guest, & Kalil, 2010; Magnuson & Votruba-Drzal, 2008; Raphael, 2011), but, to date, few have queried the human brain to assess distal, neural traces of economic conditions in childhood (Tribble & Kim, 2019). While some studies uncover a positive association between childhood SES and increased hippocampal volumes in adulthood (R. T. Staff et al., 2012), others do not (Elbejjani et al., 2017; Lawson et al., 2017).

Neuroimaging studies on the effects of SES on the human brain have traditionally assessed morphometry characteristics using surface- and voxel-based computational anatomy techniques (Noble et al., 2015; Lawson et al., 2013). Recent advances in quantitative magnetic resonance imaging (qMRI) methods allow for a more direct measurement of brain tissue properties that correlate with histological measures (Edwards, Kirilina, Mohammadi, & Weiskopf, 2018; Weiskopf, Mohammadi, Lutti, & Callaghan, 2015). Specifically, qMRI provides access to brain tissue properties—myelin, iron, and tissue water—that correlate with histological measures. Beyond this, relaxometry-based qMRI minimizes spurious findings in voxel- and surface-based morphometry related to spatially distributed intracortical myelin and iron (Lorio et al., 2016; Natu et al., 2019; Taubert et al., 2020). Thus, qMRI can be used to measure brain tissue properties with an enhanced precision relative to traditional anatomical MRI measures (Tabelow et al., 2019; Trofimova et al., 2021).

Another feature of neuroimaging studies on SES is their focus on gray matter to detect the effects of exogenous variables on neural differences, but white matter may be more susceptible to plastic changes in adulthood (Fields & Bukalo, 2020) and therefore especially pertinent to neural correlates of social adversity (Chahal, Kirshenbaum, Ho, Mastrovito, & Gotlib, 2021). While some have sought SES-related white matter differences in children (Ozernov-Palchik et al., 2019) and adults (Johnson, Kim, & Gold, 2013), they have primarily employed tensor-based models of diffusion-weighted imaging. Tensor-based measures of white matter microstructure lack a straightforward neuro-biological interpretation (Wozniak & Lim, 2006) and are susceptible to inter-site bias (Moyer, Steeg, Tax, & Thompson, 2020). Noninvasive in vivo white matter assessment remains a challenging endeavor (Heath, Hurley, Johansen-Berg, & Sampaio-Baptista, 2018) but magnetization-transfer (MT) saturation offers a reliable marker of myelin content (Mancini et al., 2020; Melie-Garcia et al., 2018; Natu et al., 2019). MT refers to the magnetization exchange between free protons and those bound to macromolecules such as myelin (Wolff & Balaban, 1994). While diffusion imaging indexes myelin via the movement of water in fiber tracts and is thus susceptible to several sources of measurement error (Tax et al., 2019), MT saturation maps quantify microstructural properties that are both sensitive and specific to the myelin fraction, rendering inter-site variability low (Gracien et al., 2020). Imaging studies have found MT saturation correlates to ex-vivo histological assessment of myelin in postmortem brains (Schmierer, Scaravilli, Altmann, Barker, & Miller, 2004; West et al., 2018), and, in addition, have the added benefit of being less susceptible to inter-site variance (Lutti, Dick, Sereno, & Weiskopf, 2014). MT saturation's enhanced myelin sensitivity relative to diffusion imaging may therefore better serve in highlighting myelin variation in a population cohort, where differences are expected to be subtle.

In this study, we aimed to identify a neural embedding of childhood SES in an older population. To that end, we probed potential differences in gray matter and myelin content that correspond to SES variability in a population cohort of older adults, using quantitative MRI (Tabelow et al., 2019). We hypothesize that childhood SES will be

reflected in late-life neural markers even when adjusting for SES in adulthood. We investigate these differences at both the whole-brain level, to query differences that may be evoked by qMRI's sensitivity; and also probe the hippocampus as an a priori ROI. We query this hypothesis by analyzing a large population cohort ($n = 1{,}166$) of older adults (mean age = 59.65 years) from one scanner site; employing quantitative neuroimaging using multiparametric maps; applying a data-driven measure of SES; and exploiting a reliable marker of myelin. We further hypothesize that such differences will be observed in both gray and white matter, as quantified by MT saturation mapping. While previous studies have found mixed results regarding later-life neural markers of childhood socioeconomic conditions, the characteristics of a large qMRI dataset may yet identify associated brain markers.

## 2 | METHODS AND MATERIALS

### 2.1 | Cohort

The study sample (BrainLaus) is a nested neuroimaging project within the CoLaus|PsyCoLaus general population cohort of the city of Lausanne, Switzerland (Firmann et al., 2008; Preisig et al., 2009). Specifically, the BrainLaus sample consists of CoLaus participants that were both eligible and willing to undergo MRI scanning. The BrainLaus study aims to scan participants at two time points, spaced 5 years apart. These two time points represent the third and fourth study time points of the greater CoLaus study. Analyses were performed on imaging data acquired between 2014 and 2018 and represented the first BrainLaus time point. A total of 1,274 participants were scanned at a single MRI site (Figure 1a).

### 2.2 | Cohort description

The CoLaus|PsyCoLaus study was designed to recruit a representative sample of the general population (Firmann et al., 2008). We sought to determine if the BrainLaus subset differed from the rest of the cohort on a number of key dimensions by examining differences between CoLaus|PsyCoLaus participants that were not included in the BrainLaus cohort ($n = 5{,}401$); and the BrainLaus cohort on all measures available for somatic variables ($n = 1{,}274$). (A full list of variables can be found in Appendix A). There was no significant difference in sex, education level, or last known occupation distributions between the two cohorts. We found a significant difference in age between the two cohorts, with an average age of 63 for CoLaus|PsyCoLaus participants without MRI scan and 59 for BrainLaus participants (Cohen's $d = 0.4$). This result underlines the necessity of including age as a nuisance variable in subsequent neuroimaging analyses that refer to epidemiological results drawn from the CoLaus|PsyCoLaus cohort (Figure 1b).

### 2.3 | MRI data acquisition

The scanning protocol included a multiparameter mapping (MPM) relaxometry protocol (Taubert et al., 2020) and diffusion-weighted acquisition that was not used in the current study. Approximate total scan duration lasted 4 ~ 5 min. Analyses were performed in SPM12 (http://www.fil.ion.ucl.ac.uk/spm/) using Matlab, 2017. Socioeconomic data were missing for 16 of the $n = 1{,}182$ participants whose neuroimaging data were retained. A total of $n = 1{,}166$ participants (mean age: 59.65 years; 622 females, 544 males) were included in our analyses.

Quantitative MT maps were calculated using a multi-echo 3D FLASH (fast low angle shot) protocol at a 1 mm, isotropic resolution (Weiskopf et al., 2013). The MRI data was acquired with T1-, PD-, and MT-weighted contrast (respective repetition time/flip angle [FA] of 23.7 ms/21°C, 23.7 ms/6°C, and 23.7 ms/6°C [MT]). For the MT-weighted contrast, an off-resonance Gaussian MT saturation RF pulse (4 ms, FA = 220°C, 2 KHz frequency offset) was applied before non-selective excitation. Multiple echo images were acquired with echo times ranging from 2.2 to 19.7 ms (except for the MT-weighted scans

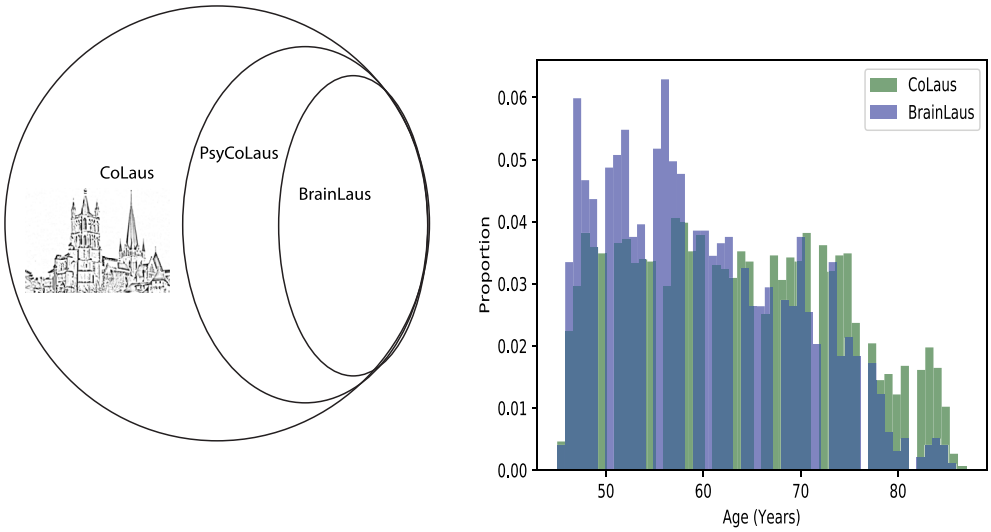


**FIGURE 1** Cohort characteristics. (a) The BrainLaus study comprises a subset of the PsyCoLaus cohort, which is itself a subset of the population cohort (Cohorte Lausanne, CoLaus). (b) The CoLaus Cohort includes a representative sample of the population, which is reflected in the BrainLaus subset, but for age. Here, age distributions for participants in the BrainLaus study are shown alongside age distributions for participants that did not undergo MR scanning

where the maximum echo time was 17.2 ms, due to the application of the MT saturation pulse). We used GRAPPA parallel imaging (acceleration factor of 2) in anterior–posterior phase encoding direction and 6/8 partial Fourier acquisitions in the partition direction (left–right). The protocol also included the acquisition of MRI data for the mapping of the radio-frequency excitation field B1 (Lutti et al., 2014). This data was acquired using the technique described in (Lutti et al., 2012). Acquisition settings were identical to those described in (Taubert et al., 2020).

## 2.4 | MRI data preprocessing

Acquired MRI data underwent automated preprocessing in the multichannel unified segmentation Bayesian framework of SPM12 yielding GM and WM probability maps derived from MT and PD* maps. To achieve higher anatomical precision, we used additionally the diffeomorphic spatial registration DARTEL based on all individual GM and WM tissue maps (Ashburner & Friston, 2005) to then apply the derived spatial registration parameters onto gray matter volume and MT saturation maps and warp these to standard MNI space. Aiming to preserve the initial total MT saturation signal, we followed the default settings for implementation of an established weighted-averaging procedure using in-house software tools (Draganski et al., 2011 ).

## 2.5 | Image quality assessment

Data quality assessment in neuroimaging is a crucial antecedent to data analysis (Alfaro-Almagro et al., 2018; Esteban et al., 2017). Given the size and average age of the cohort, as well as the plurality of MRI data acquired, a multistep image quality procedure was applied to our initial sample of $n = 1{,}274$. In a first instance, we computed regional averages for MT, R2*, and gray matter volumes for each participant by applying individual inverse deformation fields to anatomical derived from the MICCAI 2012 Grand Challenge and Workshop on Multi-Atlas Labeling (https://my.vanderbilt.edu/masi/about-us/resources-data), yielding 129 values for each participant, for each dataset. Individual average values falling outside a range of ±4 SDs from the group mean of a specific brain region were flagged ($n = 55$). In a second instance, we examined differences between individual GM, WM, and CSF segmentations and corresponding canonical tissue probability maps. We first binarized individual tissue segmentations before conducting this procedure. Resulting images were then vectorized, assigned a value of 1 for all voxels >0 and summed. Participants for whom this total difference exceeded the group's average difference by 2 SDs were subsequently flagged ($n = 31$). Finally, we performed a visual inspection of datasets that showed high SDs of the R2* parameter in white matter. This index has been shown to exhibit a high correlation with motion history during data acquisition (Castella et al., 2018). The criterion for a high SD was set to a conservative cut-off, which flagged approximately 500 potentially problematic datasets. As our cohort tended toward an older population, we expect more movement than average. Therefore, we visually examined these 500 datasets to identify gross movement, physiological anomalies, or other artifacts. This visual rating identified $n = 25$ problematic datasets. Neuroimaging datasets that failed one or more of the above quality check were excluded from analysis ($n = 80$). An additional six participants did not have complete neuroimaging datasets, and a further six were found to have been scanned with a different head coil and were also excluded from the data analysis pool. Finally, SES data were missing for $n = 16$ of the retained neuroimaging datasets, leaving a total of $n = 1{,}166$ participants included in the final analysis (Appendix D).

## 2.6 | Neuroimaging data analysis

Analyses were performed in SPM12, using Matlab, 2017. We designed three multiple regression analyses in SPM for each neuroimaging dataset to examine brain differences linked to SES in the cohort. In the first two models (Model 1 and Model 2), we included either adult SES (aSES) or childhood SES (cSES) as a covariate of interest. For the third (Model 3), we designed a full model that included both aSES and cSES. By including the two SES variables, we can assess the unique contribution of one or the other to neural outcome variables. Importantly, we did not orthogonalize these two measures as no firm principle can attribute primacy to one or the other. Finally, age, sex, and total intracranial volume (TIV)—a proxy for head size—were included in the design as nuisance variables (Peelle, Cusack, & Henson, 2012).

Our approach to statistical analysis was informed by a desire to balance both Type I and Type II errors (Eklund, Nichols, & Knutsson, 2016; Kang, Blume, Ombao, & Badre, 2015; Noble, Scheinost, & Constable, 2020). Therefore, we performed both whole-brain and ROI analyses, detailed below. We tested for the overall contribution of SES to differences in neural data by estimating coefficients using threshold-free cluster enhancement (TFCE) and applying nonparametric tests (5,000 permutations) to probe for significance (Smith & Nichols, 2009). Analyses were performed with a significance threshold of $p = 0.05$, FWE corrected for multiple comparisons across the whole search volume, comprising either the brain's entire gray matter or white matter (Ashburner & Friston, 2005). For the whole brain analysis, we report TFCE and t-statistic results that survive FWE correction with a threshold of $p = 0.05$.

In a second instance, we performed a small volume correction (SVC) analysis focusing on the hippocampus, a region that consistently emerges in studies probing the neural correlates of SES (Hanson et al., 2011; Jednoróg et al., 2012; Ursache & Noble, 2016; Elbejjani et al., 2017; Piras, Cherubini, Caltagirone, & Spalletta, 2011; Yaple & Yu, 2020; R. T. Staff et al., 2012; Lawson, Mathys, & Rees, 2017) in Model 3. Coefficients were estimated using the TFCE methods applied to a hippocampal mask comprised of left and right hippocampi. We constrained our a priori region set to the hippocampus to minimize the risk of errors of reverse inference (Poldrack, 2011).

Regional masks applied in the SVC analysis were derived from the MICCAI 2012 Grand Challenge and Workshop on Multi-Atlas Labeling (https://my.vanderbilt.edu/masi/about-us/resources-data).

### 2.7 | SES variables

The CoLaus|PsyCoLaus longitudinal cohort study collected a wide range of sociodemographic variables from which we derived SES measures. SES can be indexed in several ways; however, consensus holds that three observable variables can serve as valid measures of the underlying construct, namely, education, income, and occupation levels (Winkleby, Jatulis, Frank, & Fortmann, 1992; Oakes & Rossi, 2003). Because SES is a multifactorial construct, it is commonly indexed by composite measures (Shavers, 2007; Mueller & Parcel, 1981; Stumm et al., 2020) that can be weighted empirically before being aggregated into one score (Cowan et al., 2012; United Nations Economic Commission for Europe, 2018). In this study, we focused on the above three facets of SES to construct a composite measure. CoLaus|PsyCoLaus demographic data included information on mean income (in six intervals), education (three levels), and self and partner's last known occupation. Education levels were ranked according to highest level completed in the following manner: mandatory school or apprenticeship (low); high school diploma or upper secondary education (middle); and university degree and above (high). Occupations were ranked according to the European Socioeconomic Classification (ESEC) scale (https://www.iser.essex.ac.uk/archives/esec/user-guide) (nine levels) and assigned a corresponding numerical value; own income was taken to be highest household income between spouses, where applicable. Measures of childhood SES included father's occupation (ranked according to the ESEC scale); highest parental education (three levels); and a measure of childhood household financial status as proxy of childhood income (Appendix B). This last measure included a sum of nine positive and negative answers for family lifestyle and conditions, such as ownership of a car and having insufficient heating. The following variables were scaled into tertiles and assigned values ranging from 0 to 2. Adult occupation, taken as highest household occupation, mean income, paternal occupation, and childhood finances. To further obtain a precise, data-driven measure of adult and childhood SES constructs specific to our cohort, we extracted variance contributions from each of the SES components listed by performing two PCAs for the trio of adult and childhood SES variables. We found that, in adulthood, education explained most of the variance (63.7%), followed by income (21.84%) and occupation (14.5%). In childhood, household income explained most of the variance (70.39%), followed by education (16%) and occupation (13.6%). We then created a composite measure of adult SES and one of childhood SES by weighting tertile measures of income, education, and occupation with their respective variance contributions before summing them. This procedure allowed for the range of possible SES variables to increase from 3 to 48, with a concomitant increase in information, as formalized by entropy, from 1.58 to 4.68 and 1.55 to 3.67 bits, for adult and childhood SES, respectively. By weighting the SES composite measure components by their respective variance weights, we produced a single, precise, sample-specific measure of SES to include as an independent variable in our analyses (see Appendix E for analyses on unweighted composite SES).

## 3 | RESULTS

There was no significant difference in sex, education level, or last known occupation distributions between the CoLaus|PsyCoLaus and the BrainLaus subsample. We found a significant difference in age between the two subsamples, with an average age of 63 for CoLaus|PsyCoLaus participants without MRI scan and 59 for BrainLaus participants (Cohen's $d = 0.4$). This result underlines the necessity of including age as a nuisance variable in subsequent neuroimaging analyses that refer to epidemiological results drawn from the CoLaus|PsyCoLaus cohort (Figure 1b).

### 3.1 | Model 1—Brain differences associated with adult SES

#### 3.1.1 | MT differences associated with adult SES

Adult SES was tied to decreases in MT density in the right entorhinal cortex (Table 1; Figure 2).

#### 3.1.2 | Gray matter volume differences associated with adult SES

Adult SES correlated positively with gray matter volume in several regions, including right postcentral gyrus, left precuneus, left thalamus, and right cerebellum (exterior) (Table 1; Figure 2). SVC analyses on the hippocampus reveal greater bilateral gray matter in association with SES (Table 4).

We also probed the possible interaction of SES with age to query a differential aging effect modulated by SES (Steptoe & Zaninotto, 2020), but found no results in either MT or gray matter, when correcting for multiple comparisons.

### 3.2 | Model 2—Brain differences associated with childhood SES

#### 3.2.1 | MT changes associated with childhood SES

Childhood SES (cSES) correlated significantly positively with MT in right superior parietal lobule. In white matter, cSES correlated positively with MT near the pallidum/ventral tegmentum and bilateral precentral gyrus (Table 2). The pattern found in MT notably delineates the sensorimotor network (van den Heuvel & Hulshoff Pol, 2010) (Table 2; Figure 3).

**TABLE 1** Whole brain voxel level analysis of MT load and gray matter in relation to adult SES (aSES)

| Region | Cluster size k | p(FWE-corr) | t | Coordinates | | |
|---|---|---|---|---|---|---|
| | | | | x | y | z mm |
| MT aSES negative correlation | | | | | | |
| R Entorhinal cortex | 73 | 0.005 | 4.84 | 20 | 0 | −45 |
| **Region** | **Cluster size k** | **p(FWE-corr)** | **TFCE** | **Coordinates** | | |
| **GM aSES positive correlation** | | | | **x** | **y** | **z mm** |
| L thalamus | 13,311 | 0.001 | 2147.37 | −12 | −22 | −8 |
| | | 0.001 | 2093.13 | −18 | −24 | −18 |
| | | 0.001 | 2043.74 | 0 | −27 | −12 |
| L precuneus | 2,692 | 0.003 | 1683.40 | −6 | −54 | 72 |
| | | 0.005 | 1660.89 | −8 | −50 | 63 |
| | | 0.012 | 1408.12 | 9 | −52 | 74 |
| R cerebellum | 1,665 | 0.010 | 1429.71 | 34 | −75 | −56 |
| | | 0.027 | 1190.74 | 42 | −78 | −44 |
| R middle occipital gyrus | 237 | 0.047 | 1070.21 | 45 | −82 | 20 |
| | | 0.048 | 1061.22 | 34 | −92 | 10 |
| | | 0.050 | 1035.24 | 39 | −92 | 3 |
| R cerebellum exterior | 54 | 0.049 | 1040.59 | 15 | −62 | −62 |
| L postcentral gyrus | 11 | 0.050 | 1030.87 | −24 | −28 | 74 |
| | 6 | 0.050 | 1029.47 | −15 | −34 | 78 |

*Note*: Results shown above are significant at a threshold of p = 0.05, FWE corrected for multiple comparison using the TFCE method.
Abbreviations: GM, gray matter; MT, magnetization transfer.

#### 3.2.2 | Gray matter volume differences associated with childhood SES

Childhood SES correlated positively with gray matter volume in several regions, including right cerebellum, left postcentral gyrus, right lingual gyrus, brainstem, left precentral gyrus, left inferior temporal gyrus, and left occipital fusiform gyrus (Table 2; Figure 3). SVC analyses reveal significant associations with cSES in the left hippocampus (Table 4).

As with adult SES, no results emerged for an age by childhood SES interaction in either MT or gray matter, when correcting for multiple comparisons.

### 3.3 | Model 3—Full model

To better inform our hypothesis, we further analyzed both child- and adulthood-SES in the same model. These two variables are significantly correlated ($r = 0.536$, $p < 0.001$), and thus we computed their variance inflation factor (VIF) to determine if the presence of multicollinearity could be tolerated, finding a value of 1.40, which falls below a conservative cutoff of 5 (Mumford, Poline, & Poldrack, 2015). At the whole brain level, significant results were found for positive associations between childhood SES and MT in the left pallidum and precentral gyrus, and gray matter in bilateral cerebellum, left cuneus, left postcentral gyrus and right thalamus, and middle temporal gyrus (Table 3; Figure 4).

#### 3.3.1 | Small volume correction analysis, model 3—Adult SES

SES correlated positively with the left hippocampus gray matter volume (Table 4).

#### 3.3.2 | Small volume correction analysis, model 3—Childhood SES

Childhood SES correlated positively with the left hippocampus in white matter. Childhood SES further correlated negatively with right hippocampal volume (Table 4).

## 4 | DISCUSSION

In this study, we examined the relationship between life-course SES and structural brain properties using MRI-derived estimates indicative

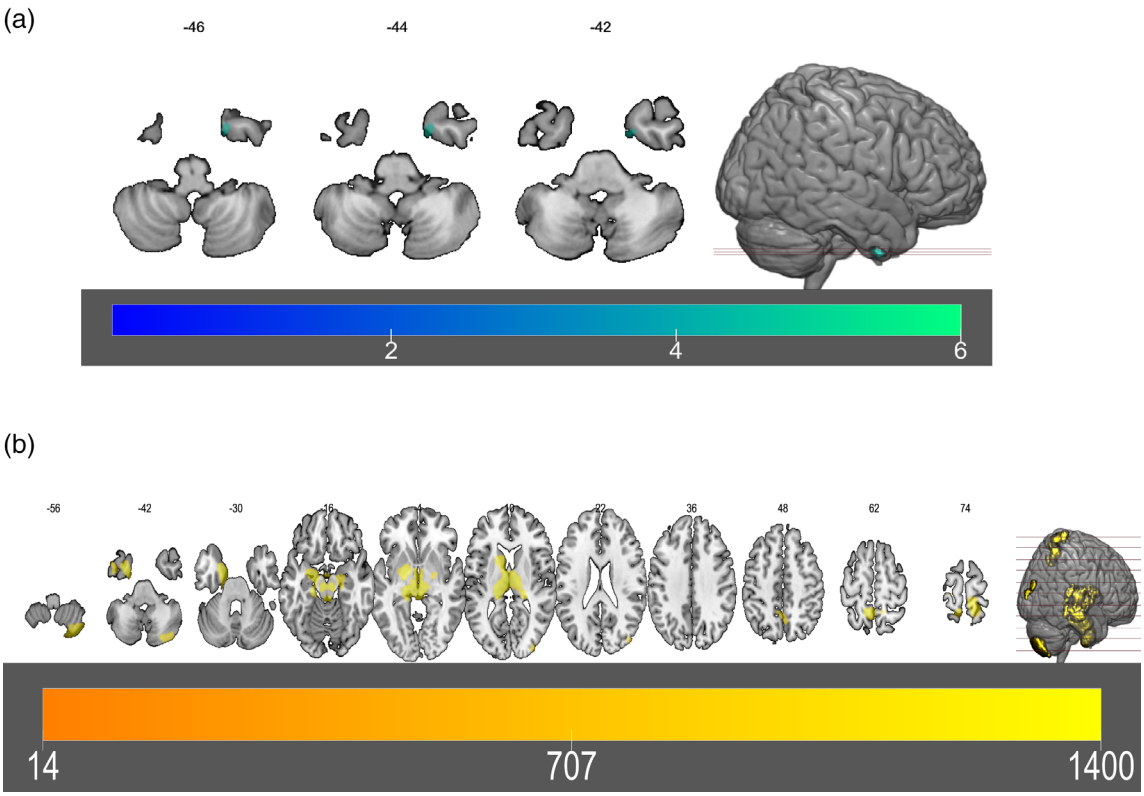


**FIGURE 2** Results of GLM 1 (adult SES). (a) Results of a negatively signed one-sample *t* test (*t*-statistic) of adult SES on MT. (b) Results of a positively signed one-sample *t* test of adult SES on gray matter volume (TFCE). Colorbars indicate *t* values. All maps shown are thresholded at $p = 0.05$, FWE-corrected for multiple comparisons

of myelin content and gray matter volume in mid- and old-age individuals from the general population. In contrast to previous studies, we adopted a life-course perspective and hypothesized that neural traces of childhood SES remain when controlling for adult SES. We found that both childhood and adult SES separately correlated with gray matter volume and myelin differences. The effect of childhood SES on gray matter volume and myelin content was independent of adult SES circumstances. Childhood SES was associated with robust neural differences even when controlling for adult SES. Our results support the hypothesis that childhood SES leaves a neural imprint even in adulthood and more generally, corroborate the latent effect model for the impact of childhood SES on adult outcomes (Nelson & Gabard-Durnam, 2020).

Studies on neural imprints of SES have yielded variable results, as highlighted in a recent meta-analysis (Yaple & Yu, 2020), which may be due in part to limited sample sizes and acquisitions across different sites. Two key studies have attempted to overcome this problem (Noble et al., 2015; McDermott et al., 2019), finding, in the first, a positive correlation between parental education and hippocampal volume, without adjusting for family income, and an association between cortical surface area and both parental income and education. In the second study, widespread cortical surface area and hippocampus similarly correlate with higher SES, as assessed by the Hollingshead score. While these two studies yield concordant results, they are both found in pediatric cohorts and do not investigate white matter measures. Our results support hippocampal involvement in SES differences, with higher bilateral hippocampal gray matter correlating with higher adult SES. However, only left hippocampal gray matter and myelin correlated with childhood SES; right hippocampal gray matter displayed a negative association with childhood SES, and at the same time, a positive association between MT and the same variable. This discrepancy in the relationship between hippocampus and SES may highlight a specificity in effects on brain tissue properties, as hippocampal volume may cede to increases in myelination (Natu et al., 2019).

An innovative feature of our study is the use of MT saturation maps to extract estimates of gray matter volumes (Helms, Draganski, Frackowiak, Ashburner, & Weiskopf, 2009) and myelin content (Melie-Garcia et al., 2018), which in part serves to dampen scanner site variability (Focke et al., 2011; Gracien et al., 2020). Our results therefore offer an added reliability over findings obtained with traditional MRI methods, particularly with regards to myelin quantification methods. Further, myelin may be a more pertinent metric for function across the lifespan (Ziegler et al., 2019; Chen, Chen, Hsu, & Tseng, 2020).

### 4.1 | SES differences in brain's myelin

Most studies on in vivo structural brain properties linked to SES focus on gray matter volume or cortical thickness measures. However,

**TABLE 2** Whole brain voxel level analysis of MT load and gray matter volumes in relation to childhood SES (cSES)

| Region | Cluster size k | p(FWE-corr) | t | Coordinates | | |
|---|---|---|---|---|---|---|
| | | | | *x* | *y* | *z* mm |
| MT CSES positive correlation | | | | | | |
| R superior parietal lobule | 40 | 0.006 | 4.77 | 21 | −45 | 68 |
| **Region** | **Cluster size k** | **p(FWE-corr)** | **TFCE** | **Coordinates** | | |
| **MT CSES positive correlation** | | | | *x* | *y* | *z* mm |
| R Precentral gyrus | 35,076 | 0.010 | 1729.76 | 22 | −26 | 68 |
| | | 0.010 | 1725.54 | 15 | −28 | 70 |
| | | 0.010 | 1717.47 | 9 | −30 | 76 |
| L precentral gyrus | 10,208 | 0.013 | 1542.19 | −14 | −16 | 72 |
| | | 0.017 | 1472.27 | −30 | −24 | 58 |
| | | 0.017 | 1461.96 | −18 | −28 | 68 |
| L pallidum | 1,435 | 0.025 | 1312.31 | −14 | 0 | −6 |
| | | 0.025 | 1305.36 | −3 | 0 | −3 |
| | | 0.038 | 1138.80 | −20 | −3 | 3 |
| R inferior temporal gyrus | 1,429 | 0.034 | 1187.24 | 58 | −40 | −16 |
| | | 0.034 | 1178.01 | 63 | −22 | −16 |
| | | 0.034 | 1177.60 | 62 | −33 | −15 |
| L middle frontal gyrus | 534 | 0.047 | 1056.57 | −30 | 26 | 16 |
| | | 0.047 | 1045.03 | −26 | 32 | 6 |
| | | 0.050 | 1024.23 | −42 | 22 | 26 |
| MT CSES negative correlation | | | | | | |
| R temporal pole | 7 | 0.035 | 4.48 | 21 | 8 | −45 |
| GM CSES positive correlation | | | | | | |
| R cerebellum | 75,617 | 0.001 | 3478.54 | 18 | −62 | −62 |
| | | 0.001 | 3435.18 | −34 | −75 | −54 |
| | | 0.001 | 3431.38 | −21 | −58 | −62 |
| L postcentral gyrus | 19,385 | 0.001 | 2365.76 | −9 | −34 | 78 |
| | | 0.001 | 2289.61 | 9 | −40 | 78 |
| | | 0.001 | 2261.26 | −21 | −30 | 75 |
| L inferior temporal gyrus | 617 | 0.019 | 1159.46 | −22 | −6 | −50 |
| | | 0.043 | 1019.08 | −38 | 2 | −48 |
| | | 0.048 | 987.69 | −15 | 0 | −44 |
| R occipital fusiform gyrus | 34 | 0.043 | 1013.19 | 24 | −70 | −14 |
| R posterior cingulate gyrus | 1 | 0.043 | 1009.62 | 9 | −51 | −27 |

*Note*: Results shown above are significant at a threshold of $p = 0.05$, FWE corrected for multiple comparison using the TFCE method.
Abbreviations: GM, gray matter; MT, magnetization transfer.

myelin plays a crucial role in brain function and dysfunction (Fields & Bukalo, 2020) and therefore should not be neglected. As shown in our study, MT values covaried with SES in regions distinct from gray matter volume changes, highlighting myelin's independent status in the brain. Our results support a recent study showing a relationship between neighborhood deprivation, and rate of myelination, as assessed by MT, across childhood and adolescence (Ziegler et al., 2019). Further, we find a positive association of myelin in regions comprising the sensorimotor network with SES. This network has previously been associated to cognitive impairment (Agosta et al., 2010) and MT in old age correlated with motor performance (Seidler et al., 2015). Aging induces cognitive decline (Park, O'Connell, & Thomson, 2003), even in early adulthood (Salthouse, 2009) as well as decreases in motor performance (Thompson, Blair, & Henrey, 2014). Converging evidence highlights the increasing association between cognitive and sensorimotor functions with aging (Li &

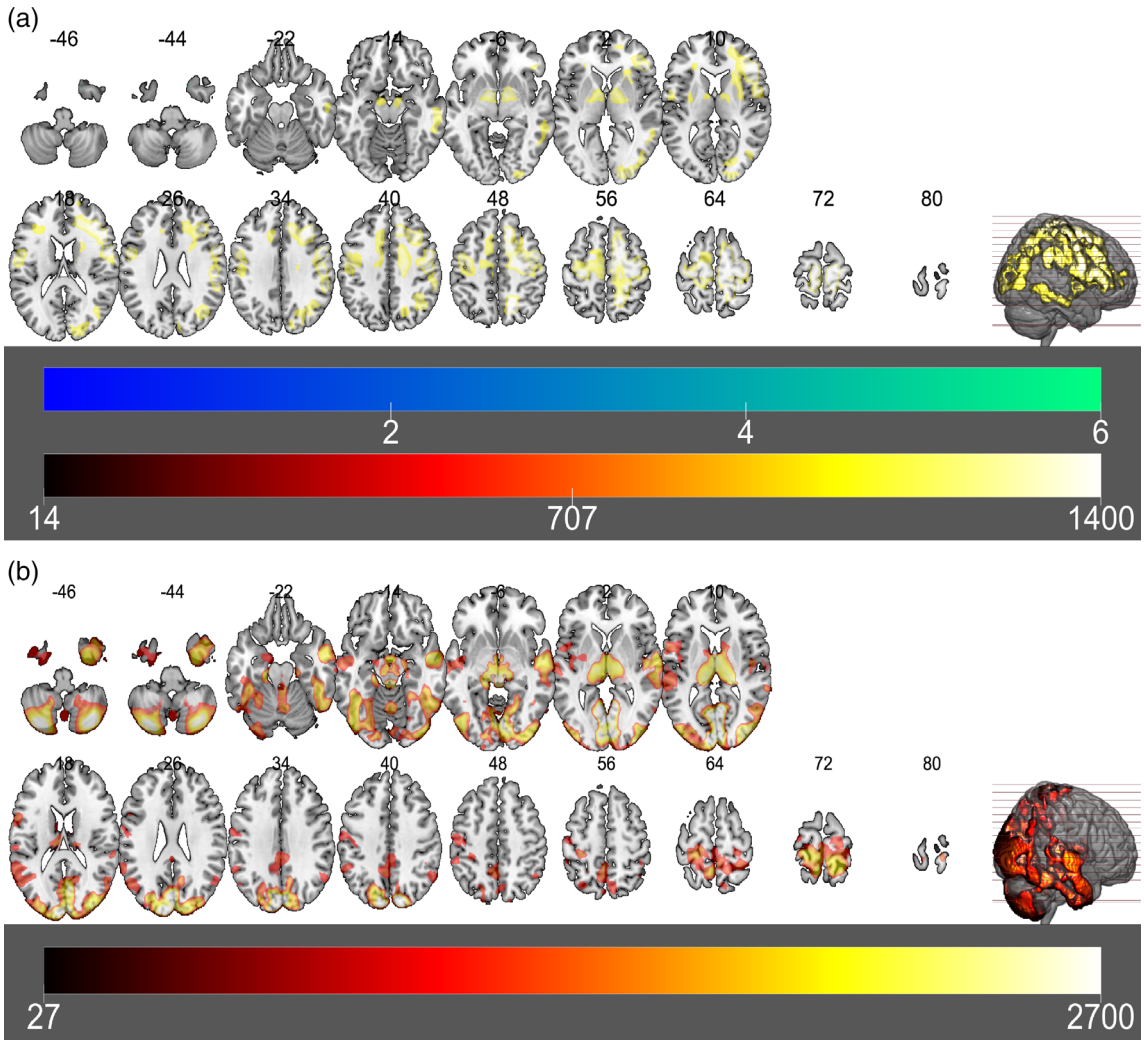


**FIGURE 3** Results of GLM 2 (Childhood SES) in MT maps and gray matter volumes. (a) Results of both positively (TFCE) and negatively (t-statistic) signed one-sample *t* tests of childhood SES on MT. (b) Results of both positive (TFCE) one-sample *t* tests on childhood SES on in gray matter. All maps shown are thresholded at $p = 0.05$, FWE-corrected for multiple comparisons

Lindenberger, 2002). One possibility is that childhood SES may provide a buffer to functional decline in old age via increased myelination of the sensorimotor network.

## 4.2 | Regional specificity of SES neural differences

Brain regions found to covary with SES play important roles in cognition, memory, and motor function. The pallidum plays a role in reward and motivation (Smith, Tindell, Aldridge, & Berridge, 2009), as well as motor function (Gillies et al., 2017). The hippocampus plays a significant role in memory (Knierim, 2015) as do regions of the temporal lobe (Wong & Gallate, 2012), also implicated in language functions (Davey et al., 2016). The hippocampus in particular has previously been found implicated in psychosocial adversity (Tottenham & Sheridan, 2009) and is also known to be especially susceptible to plasticity (Leuner & Gould, 2010). Differences in any of these structures may therefore have considerable functional implications. The nature of the study prevents claims of causality between SES and implicated regions. Further, neuroimaging studies are prone to errors of reverse inference (Poldrack, 2011). The exact biological pathway between childhood economic status and health in adulthood remains ill-defined (Matthews & Gallo, 2011; Foulkes & Blakemore, 2018). Nonetheless, we speculate that the hippocampus in particular may be related to SES by way of enriched environments in childhood (Cassarino & Setti, 2015). SES effects on hippocampal volumes in children are mediated by caregiver quality (Luby et al., 2013) and higher SES may stem stress-related effects on the hippocampus (McEwen, 2012). SES-related access to extracurricular activities in childhood and green space may also enhance cognition by way of the temporal lobe (Hillman, Erickson, & Kramer, 2008), a link that may be mediated by motor regions (Voss, Nagamatsu, Liu-Ambrose, & Kramer, 2011). SES is also related to aberrant reward responses (Hanson et al., 2016; Oshri et al., 2019), which may reflect our findings in the pallidum.

**TABLE 3** Whole brain voxel level analysis of MT and gray matter in relation to SES in a full model including both childhood and adult SES

| Region | Cluster size k | p(FWE-corr) | TFCE | Coordinates | | |
|---|---|---|---|---|---|---|
| | | | | *x* | *y* | *z* mm |
| MT cSES positive *t* test | | | | | | |
| L pallidum | 1,311 | 0.033 | 1,173.28 | −12 | −2 | −6 |
| | | 0.033 | 1,167.98 | −6 | −6 | −9 |
| | | 0.038 | 1,137.08 | −14 | −9 | −12 |
| L precentral gyrus | 992 | 0.041 | 1,086.14 | −30 | −24 | 58 |
| | | 0.041 | 1,073.47 | −15 | −16 | 68 |
| | | 0.043 | 1,056.36 | −18 | −32 | 66 |
| L precentral gyrus | 104 | 0.048 | 1,018.33 | −44 | −15 | 44 |
| | | 0.049 | 1,016.70 | −38 | −12 | 48 |
| GM cSES positive *t* test | | | | | | |
| l cuneus | 24,255 | 0.001 | 2,604.20 | −4 | −93 | 12 |
| | | 0.001 | 2,419.18 | 3 | −60 | 4 |
| | | 0.001 | 2,415.93 | −9 | −93 | 26 |
| L cerebellum | 5,861 | 0.002 | 2026.42 | −21 | −62 | −58 |
| | | 0.002 | 1938.24 | −33 | −75 | −52 |
| | | 0.030 | 1,066.86 | −46 | −64 | −34 |
| R cerebellum | 3,596 | 0.002 | 1929.93 | 20 | −60 | −62 |
| | | 0.007 | 1,469.33 | 36 | −74 | −52 |
| | | 0.007 | 1,450.83 | 27 | −72 | −52 |
| L postcentral gyrus | 663 | 0.018 | 1,252.65 | −8 | −36 | 78 |
| | | 0.022 | 1,145.61 | −21 | −32 | 75 |
| | | 0.048 | 951.81 | −30 | −33 | 58 |
| R middle temporal gyrus | 707 | 0.031 | 1,055.50 | 57 | −4 | −16 |
| | | 0.031 | 1,052.70 | 51 | −6 | −10 |
| | | 0.033 | 1,039.95 | 54 | 0 | −26 |
| Brainstem | 548 | 0.033 | 1,034.89 | 6 | −30 | −9 |
| | | 0.039 | 994.53 | −4 | −30 | −8 |
| R postcentral gyrus | 84 | 0.044 | 965.48 | 9 | −40 | 78 |
| R thalamus | 224 | 0.047 | 953.73 | 24 | −28 | 9 |
| | | 0.048 | 951.87 | 16 | −28 | 12 |
| R inferior temporal gyrus | 77 | 0.048 | 948.40 | 54 | −54 | −16 |
| L thalamus | 56 | 0.049 | 938.82 | −10 | −30 | 14 |
| R superior parietal lobule | 30 | 0.050 | 927.97 | 22 | −42 | 72 |
| R transverse temporal gyrus | 16 | 0.050 | 926.23 | 46 | −10 | 6 |

*Note*: Results shown above are significant at a threshold of $p = 0.05$, FWE corrected for multiple comparison using the TFCE method.
Abbreviations: GM, gray matter; MT, magnetization transfer.

### 4.3 | SES differences and the hippocampus

Differences in hippocampal gray matter volume associated with SES have previously been reported in a number of studies (Jednoróg et al., 2012; R. T. Staff et al., 2012). Our results partially support this relationship, but we detect an inverse relationship between right hippocampal gray matter and childhood SES. We otherwise find positive relationships between bilateral hippocampal gray matter and adult SES. Childhood SES in our cohort was nonetheless also associated negatively with MT in bilateral temporal pole, which, like the hippocampus, forms part of the temporal lobe system, and is uniquely sensitive to age-related decline (Pelletier et al., 2017). Childhood SES further correlates positively with greater MT in left hippocampus (and right hippocampal gray matter), raising the possibility of interplay between myelin and gray matter. For instance, cortical gray matter reduction occurs in healthy adolescence along with an increase of myelination (Giorgio et al., 2010). In the same model, adult SES correlated with increased left hippocampal volume. Our results thus

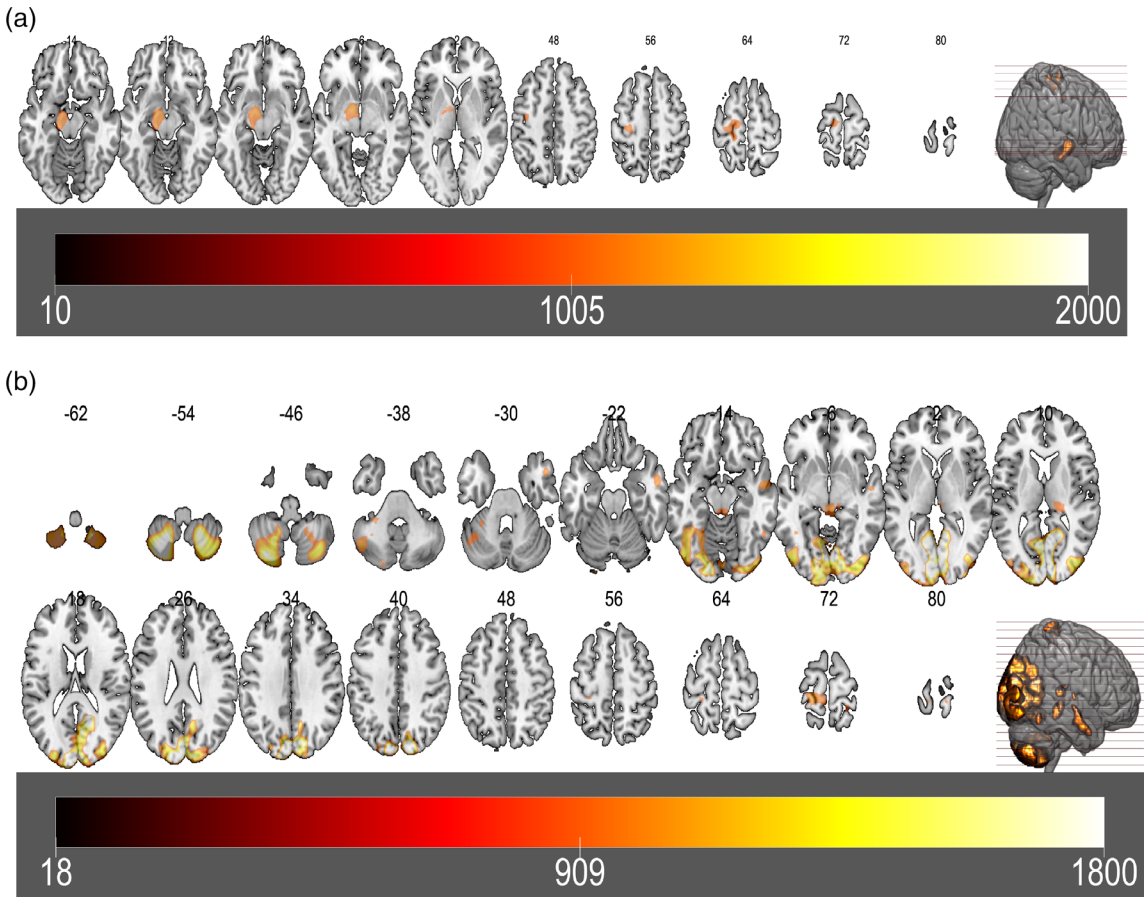


**FIGURE 4** Results of GLM 3 for childhood SES including adult and childhood SES as covariates in MT maps and gray matter volumes. (a) Results of positive childhood SES correlates in MT. (b) Results of *t* tests on childhood SES in gray matter. Colorbars indicate TFCE-values. All maps shown are thresholded at $p = 0.05$, FWE-corrected for multiple comparisons

**TABLE 4** Small volume correction analysis of MT load and gray matter volumes in relation to childhood and adult SES in Model 3

| Region | Cluster size k | p(FWE-corr) | TFCE | Coordinates | | |
|---|---|---|---|---|---|---|
| | | | | *x* | y | *z* mm |
| MT cSES | | | | | | |
| Positive *T* test | | | | | | |
| L hippocampus | 1 | 0.021 | 153.18 | −16 | −16 | −16 |
| L hippocampus | 1 | 0.022 | 151.26 | −15 | −14 | −16 |
| L hippocampus | 2 | 0.024 | 144.55 | −18 | −18 | −15 |
| L hippocampus | 1 | 0.026 | 138.78 | −18 | −14 | −14 |
| GM aSES | | | | | | |
| Positive *T* test | | | | | | |
| L hippocampus | 256 | 0.011 | 203.06 | −16 | −9 | −22 |
| L hippocampus | 3 | 0.045 | 125.61 | −20 | −27 | −10 |
| GM cSES | | | | | | |
| Negative *T* test | | | | | | |
| R hippocampus | 301 | 0.016 | 205.34 | 36 | −28 | −9 |

*Note*: TFCE analysis results constrained to an anatomical mask for the hippocampus (left and right). Results shown above are significant using a threshold of $p = 0.05$, FWE corrected for multiple comparisons constrained to the search volume.

suggest a more complex interaction in temporal lobe regions in relation to SES, with differential effects of myelin, gray matter and early or late-life SES implicated in disparate neural profiles.

### 4.4 | Limitations of the study

Here, childhood SES was assessed using adult recall that is susceptible to faulty memories (Havari & Mazzonna, 2015). Household income in childhood and adulthood are further indexed by different measures and it can be argued that the one for childhood skews towards assessing disadvantage, although this bias may be redressed as retrospective assessments tend to favor a more optimistic view of how things were (Mitchell, Thompson, Peterson, & Cronk, 1997). We also define SES with a composite measure, which does not identify unique risk factors (Hackman, Farah, & Meaney, 2010). Further, we cannot associate function to SES-related neural differences, as the current dataset does not include cognitive or behavioral variables, nor does it include mother's occupation as a potential indicator. Finally, our study design precludes the possibility to control for context beyond SES in early life that can impact neural structure. In spite of these limitations, our results are based on a precious dataset, as not all large-scale neuroimaging data have childhood, or conversely, adult data, and few include quantitative MRI maps.

## 5 | CONCLUSIONS

Our study adds to the growing literature on brain correlates of SES. Known associations between childhood adversity and late-life outcomes strongly suggest a causal process set into the arrow of time. By highlighting a neurophysiological embedding of childhood SES in old age, our results add credence to the lasting physical incorporation of exogenous social factors into the brain.

### ACKNOWLEDGMENTS

The CoLaus|PsyCoLaus study was and is supported by research grants from GlaxoSmithKline, the Faculty of Biology and Medicine of Lausanne, and the Swiss National Science Foundation (grants Nr. 3200B0_105993, 3200B0_118308, 33CSCO_122661, 33CS30_139468, and 33CS30_14840). L.L.-K. and S.S. were supported by the European Commission (H2020 Lifepath grant No. 633666), and by the Leenaards and Jeantet Foundations. B.D. is supported by the Swiss National Science Foundation (NCCR Synapsy, project grant Nr. 32003B_135679, 32003B_159780) and the Fondation Leenaards. A.L. is supported by the Swiss National Science Foundation (project grant Nr. 320030_184784) the Fondation Roger de Spoelberch. LREN is very grateful to the Roger De Spoelberch and Partridge Foundations for their generous financial support.

Open access funding enabled and organized by Projekt DEAL.

### CONFLICT OF INTEREST

The authors report no biomedical financial interests or potential conflicts of interest.

### DATA AVAILABILITY STATEMENT

De-identified MRI features that were used for the study can be provided upon request. Non-identifiable individual-level data are available for researchers who seek to answer questions related to health and disease in the context of research projects who meet the criteria for data sharing by research committees. Please follow the instructions at https://www.colaus-psycolaus.ch/ for information on how to submit an application for gaining access to CoLaus data. Code for the quality control of the dataset is available in the following GitHub repository: https://github.com/LLouedKhen/QCQA_MPM_DATA-Additional code can be made available upon request.

### ORCID

*Leyla Loued-Khenissi* https://orcid.org/0000-0003-3241-6492
*Antoine Lutti* https://orcid.org/0000-0003-3281-5477

### REFERENCES

Aartsen, M. J., Cheval, B., Sieber, S., Van der Linden, B. W., Gabriel, R., Courvoisier, D. S., … Cullati, S. (2019). Advantaged socioeconomic conditions in childhood are associated with higher cognitive functioning but stronger cognitive decline in older age. *Proceedings of the National Academy of Sciences*, *116*(12), 5478–5486.

Agosta, F., Rocca, M. A., Pagani, E., Absinta, M., Magnani, G., Marcone, A., … Filippi, M. (2010). Sensorimotor network rewiring in mild cognitive impairment and Alzheimer's disease. *Human Brain Mapping*, *31*(4), 515–525.

Alfaro-Almagro, F., Jenkinson, M., Bangerter, N. K., Andersson, J. L., Griffanti, L., Douaud, G., et al. (2018). Image processing and quality control for the first 10,000 brain imaging datasets from UKbiobank. *NeuroImage*, *166*, 400–424.

Ashburner, J., & Friston, K. J. (2005). Unified segmentation. *NeuroImage*, *26*(3), 839–851.

Cassarino, M., & Setti, A. (2015). Environment as 'brain training': A review of geographical and physical environmental influences on cognitive ageing. *Ageing Research Reviews*, *23*, 167–182.

Castella, R., Arn, L., Dupuis, E., Callaghan, M. F., Draganski, B., & Lutti, A. (2018). Controlling motion artefact levels in MR images by suspending data acquisition during periods of head motion. *Magnetic Resonance in Medicine*, *80*(6), 2415–2426.

Chahal, R., Kirshenbaum, J. S., Ho, T. C., Mastrovito, D., & Gotlib, I. H. (2021). Greater age-related changes in white matter morphometry following early life stress: Associations with internalizing problems in adolescence. *Developmental Cognitive Neuroscience*, *47*, 100899.

Chen, P.-Y., Chen, C.-L., Hsu, Y.-C., & Tseng, W.-Y. I. (2020). Fluid intelligence is associated with cortical volume and white matter tract integrity within multiple-demand system across adult lifespan. *NeuroImage*, *212*, 116576.

Cowan, C. D., Hauser, R. M., Kominski, R. A., Levin, H. M., Lucas, S. R., Morgan, S. L., & Chapman, C. (2012). *Improving the measurement of sg for the national assessment of educational progress: A theoretical foundation*. Washington, D.C.: National Center for Education Statistics.

Davey, J., Thompson, H. E., Hallam, G., Karapanagiotidis, T., Murphy, C., De Caso, I., … Jefferies, E. (2016). Exploring the role of the posterior middle temporal gyrus in semantic cognition: Integration of anterior temporal lobe with executive processes. *NeuroImage*, *137*, 165–177.

Duncan, G. J., Ziol-Guest, K. M., & Kalil, A. (2010). Early-childhood poverty and adult attainment, behavior, and health. *Child Development*, *81*(1), 306–325.

Edwards, L. J., Kirilina, E., Mohammadi, S., & Weiskopf, N. (2018). Microstructural imaging of human neocortex in vivo. *NeuroImage*, *182*, 184–206.

Eklund, A., Nichols, T., & Knutsson, H. (2016). Can parametric statistical methods be trusted for fMRI based group studies. *Proceedings of the National Academy of Sciences*, *113*(28), 7900–7905. Retrieved from http://arxiv.org/abs/1511.01863

Elbejjani, M., Fuhrer, R., Abrahamowicz, M., Mazoyer, B., Crivello, F., Tzourio, C., & Dufouil, C. (2017). Life-course socioeconomic position and hippocampal atrophy in a prospective cohort of older adults. *Psychosomatic Medicine*, *79*(1), 14–23. Retrieved from https://journals.lww.com/psychosomaticmedicine/fulltext/2017/01000/Life_Course_Socioeconomic_Position_and_Hippocampal.3.aspx

Esteban, O., Birman, D., Schaer, M., Koyejo, O. O., Poldrack, R. A., & Gorgolewski, K. J. (2017). MRIQC: Advancing the automatic prediction of image quality in MRI from unseen sites. *PLoS One*, *12*(9), e0184661.

Farah, M. J. (2017). The neuroscience of socioeconomic status: correlates, causes, and consequences. *Neuron*, *96*(1), 56–71.

Fields, R. D., & Bukalo, O. (2020). Myelin makes memories. *Nature Neuroscience*, *23*, 469–470.

Firmann, M., Mayor, V., Vidal, P. M., Bochud, M., Pécoud, A., Hayoz, D., … Vollenweider, P. (2008). The CoLaus study: A population-based study to investigate the epidemiology and genetic determinants of cardiovascular risk factors and metabolic syndrome. *BMC Cardiovascular Disorders*, *8*(1), 6.

Focke, N. K., Helms, G., Kaspar, S., Diederich, C., Tóth, V., Dechent, P., … Paulus, W. (2011). Multi-site voxel-based morphometry - Not quite there yet. *NeuroImage*, *56*(3), 1164–1170.

Foulkes, L., & Blakemore, S.-J. (2018). Studying individual differences in human adolescent brain development. *Nature Neuroscience*, *21*(3), 315–323.

Gillies, M. J., Hyam, J. A., Weiss, A. R., Antoniades, C. A., Bogacz, R., Fitzgerald, J. J., … Green, A. L. (2017). The cognitive role of the Globus Pallidus interna; insights from disease states. *Experimental Brain Research*, *235*(5), 1455–1465.

Giorgio, A., Watkins, K. E., Chadwick, M., James, S., Winmill, L., Douaud, G., … James, A. C. (2010). Longitudinal changes in grey and white matter during adolescence. *NeuroImage*, *49*(1), 94–103.

Gracien, R.-M., Maiworm, M., Brüche, N., Shrestha, M., Nöth, U., Hattingen, E., … Deichmann, R. (2020). How stable is quantitative MRI? - assessment of intra- and inter-scanner-model reproducibility using identical acquisition sequences and data analysis programs. *NeuroImage*, *207*, 116364.

Hackman, D. A., Farah, M. J., & Meaney, M. J. (2010). Socioeconomic status and the brain: Mechanistic insights from human and animal research. *Nature Reviews Neuroscience*, *11*(9), 651–659.

Hanson, J. L., Albert, D., Iselin, A.-M. R., Carré, J. M., Dodge, K. A., & Hariri, A. R. (2016). Cumulative stress in childhood is associated with blunted reward-related brain activity in adulthood. *Social Cognitive and Affective Neuroscience*, *11*(3), 405–412.

Hanson, J. L., Chandra, A., Wolfe, B. L., & Pollak, S. D. (2011). Association between income and the hippocampus. *PLoS One*, *6*(5), e18712.

Havari, E., & Mazzonna, F. (2015). Can we trust older People's statements on their childhood circumstances? Evidence from SHARELIFE. *European Journal of Population*, *31*(3), 233–257.

Heath, F., Hurley, S. A., Johansen-Berg, H., & Sampaio-Baptista, C. (2018). Advances in noninvasive myelin imaging. *Developmental Neurobiology*, *78*(2), 136–151.

Helms, G., Draganski, B., Frackowiak, R., Ashburner, J., & Weiskopf, N. (2009). Improved segmentation of deep brain grey matter structures using magnetization transfer (MT) parameter maps. *NeuroImage*, *47*(1), 194–198.

Hillman, C. H., Erickson, K. I., & Kramer, A. F. (2008). Be smart, exercise your heart: Exercise effects on brain and cognition. *Nature Reviews Neuroscience*, *9*(1), 58–65. Retrieved from https://www.nature.com/articles/nrn2298

Jednoróg, K., Altarelli, I., Monzalvo, K., Fluss, J., Dubois, J., Billard, C., … Ramus, F. (2012). The influence of socioeconomic status on children's brain structure. *PLoS One*, *7*(8), e42486.

Johnson, N. F., Kim, C., & Gold, B. T. (2013). Socioeconomic status is positively correlated with frontal white matter integrity in aging. *Age*, *35*(6), 2045–2056.

Kang, H., Blume, J., Ombao, H., & Badre, D. (2015). Simultaneous control of error rates in fMRI data analysis. *NeuroImage*, *123*, 102–113.

Kanjilal, S., Gregg, E. W., Cheng, Y. J., Zhang, P., Nelson, D. E., Mensah, G., & Beckles, G. L. A. (2006). Socioeconomic status and trends in disparities in 4 major risk factors for cardiovascular disease among US adults, 1971–2002. *Archives of Internal Medicine*, *166*(21), 2348–2355. Retrieved from https://jamanetwork.com/journals/jamainternalmedicine/fullarticle/411309

Knierim, J. J. (2015). The hippocampus. *Current Biology*, *25*(23), R1116–R1121.

Larsson, J., Solomon, S. G., & Kohn, A. (2015). ScienceDirect special issue: Review fMRI adaptation revisited. *Cortex*, *80*, 154–160.

Lawson, G. M., Camins, J. S., Wisse, L., Wu, J., Duda, J. T., Cook, P. A., … Farah, M. J. (2017). Childhood socioeconomic status and childhood maltreatment: Distinct associations with brain structure. *PLoS One*, *12*(4), e0175690.

Lawson, G. M., Duda, J. T., Avants, B. B., Wu, J., & Farah, M. J. (2013). Associations between children's socioeconomic status and prefrontal cortical thickness. *Developmental Science*, *16*(5), 641–652.

Lawson, R. P., Mathys, C., & Rees, G. (2017). Adults with autism overestimate the volatility of the sensory environment. *Nature Neuroscience*, *20*(9), 1293–1299. Retrieved from https://www.nature.com/articles/nn.4615

Leuner, B., & Gould, E. (2010). Structural plasticity and hippocampal function. *Annual Review of Psychology*, *61*(1), 111–140.

Li, K. Z., & Lindenberger, U. (2002). Relations between aging sensory/sensorimotor and cognitive functions. *Neuroscience & Biobehavioral Reviews*, *26*(7), 777–783.

Lorio, S., Kherif, F., Ruef, A., Melie-Garcia, L., Frackowiak, R., Ashburner, J., … Draganski, B. (2016). Neurobiological origin of spurious brain morphological changes: A quantitative MRI study. *Human Brain Mapping*, *37*(5), 1801–1815.

Luby, J., Belden, A., Botteron, K., Marrus, N., Harms, M. P., Babb, C., … Barch, D. (2013). The effects of poverty on childhood brain development: The mediating effect of caregiving and stressful life events. *JAMA Pediatrics*, *167*(12), 1135–1142.

Lutti, A., Dick, F., Sereno, M. I., & Weiskopf, N. (2014). Using high-resolution quantitative mapping of R1 as an index of cortical myelination. *NeuroImage*, *93*, 176–188.

Lutti, A., Stadler, J., Josephs, O., Windischberger, C., Speck, O., Bernarding, J., … Weiskopf, N. (2012). Robust and fast whole brain mapping of the RF transmit field B1 at 7T. *PLoS One*, *7*(3), e32379.

Magnuson, K. A., & Votruba-Drzal, E. (2008). *Enduring influences of childhood poverty*. University of Wisonsin-Madison: Institute for Research on Poverty.

Mancini, M., Karakuzu, A., Cohen-Adad, J., Cercignani, M., Nichols, T. E., & Stikov, N. (2020). An interactive meta-analysis of MRI biomarkers of myelin. *eLife*, *9*, e61523.

Marmot, M., & Bell, R. (2012). Fair society, healthy lives, public health. *Public Health*, *126*, S4–S10.

Matthews, K. A., & Gallo, L. C. (2011). Psychological perspectives on pathways linking socioeconomic status and physical health. *Annual Review of Psychology*, *62*(1), 501–530.

Mayeda, E. R., Glymour, M. M., Quesenberry, C. P., & Whitmer, R. A. (2016). Inequalities in dementia incidence between six racial and ethnic groups over 14 years. *Alzheimer's & Dementia*, *12*(3), 216–224.

McDermott, C. L., Seidlitz, J., Nadig, A., Liu, S., Clasen, L. S., Blumenthal, J. D., … Raznahan, A. (2019). Longitudinally mapping childhood socioeconomic status associations with cortical and subcortical

morphology. *Journal of Neuroscience*, *39*(8), 1365–1373. Retrieved from https://www.jneurosci.org/content/39/8/1365

McEwen, B. S. (2012). Brain on stress: How the social environment gets under the skin. *Proceedings of the National Academy of Sciences*, *109*-(Suppl 2), 17180–17185. Retrieved from https://www.pnas.org/content/109/Supplement_2/17180

Melie-Garcia, L., Slater, D., Ruef, A., Sanabria-Diaz, G., Preisig, M., Kherif, F., … Lutti, A. (2018). Networks of myelin covariance. *Human Brain Mapping*, *39*(4), 1532–1554.

Merz, E. C., Maskus, E. A., Melvin, S. A., He, X., & Noble, K. G. (2020). Socioeconomic disparities in language input are associated with children's language-related brain structure and reading skills. *Child Development*, *91*, 846–860.

Mitchell, T. R., Thompson, L., Peterson, E., & Cronk, R. (1997). Temporal adjustments in the evaluation of events: The "rosy view". *Journal of Experimental Social Psychology*, *33*(4), 421–448.

Moriguchi, Y., & Shinohara, I. (2019). Socioeconomic disparity in prefrontal development during early childhood. *Scientific Reports*, *9*(1), 2585.

Moyer, D., Steeg, G. V., Tax, C. M. W., & Thompson, P. M. (2020). Scanner invariant representations for diffusion MRI harmonization. *Magnetic Resonance in Medicine*, *84*(4), 2174–2189.

Mueller, C. W., & Parcel, T. L. (1981). Measures of socioeconomic status: Alternatives and recommendations. *Child Development*, *52*(1), 13–30. Retrieved from https://www.jstor.org/stable/1129211

Mumford, J. A., Poline, J.-B., & Poldrack, R. A. (2015). Orthogonalization of regressors in fMRI models. *PLoS One*, *10*(4), e0126255.

Natu, V. S., Gomez, J., Barnett, M., Jeska, B., Kirilina, E., Jaeger, C., … Grill-Spector, K. (2019). Apparent thinning of human visual cortex during childhood is associated with myelination. *Proceedings of the National Academy of Sciences*, *116*(41), 20750–20759.

Nelson, C. A., & Gabard-Durnam, L. J. (2020). Early adversity and critical periods: Neurodevelopmental consequences of violating the expectable environment. *Trends in Neurosciences*, *43*(3), 133–143. Retrieved from https://www.cell.com/trends/neurosciences/abstract/S0166-2236(20)30003-5

Noble, K. G., Farah, M. J., & McCandliss, B. D. (2006). Socioeconomic background modulates cognition-achievement relationships in reading. *Cognitive Development*, *21*(3), 349–368.

Noble, K. G., Houston, S. M., Brito, N. H., Bartsch, H., Kan, E., Kuperman, J. M., … Sowell, E. R. (2015). Family income, parental education and brain structure in children and adolescents. *Nature Neuroscience*, *18*(5), 773–778. Retrieved from http://www.nature.com/articles/nn.3983

Noble, S., Scheinost, D., & Constable, R. T. (2020). Cluster failure or power failure? Evaluating sensitivity in cluster-level inference. *Neuroimage*, *209*, 116468.

Oakes, J. M., & Rossi, P. H. (2003). The measurement of SES in health research: Current practice and steps toward a new approach. *Social Science & Medicine (1982)*, *56*(4), 769–784.

Oshri, A., Hallowell, E., Liu, S., MacKillop, J., Galvan, A., Kogan, S. M., & Sweet, L. H. (2019). Socioeconomic hardship and delayed reward discounting: Associations with working memory and emotional reactivity. *Developmental Cognitive Neuroscience*, *37*, 100642.

Ozernov-Palchik, O., Norton, E. S., Wang, Y., Beach, S. D., Zuk, J., Wolf, M., … Gaab, N. (2019). The relationship between socioeconomic status and white matter microstructure in pre-reading children: A longitudinal investigation. *Human Brain Mapping*, *40*(3), 741–754.

Park, H. L., O'Connell, J. E., & Thomson, R. G. (2003). A systematic review of cognitive decline in the general elderly population. *International Journal of Geriatric Psychiatry*, *18*(12), 1121–1134.

Peelle, J. E., Cusack, R., & Henson, R. N. (2012). Adjusting for global effects in voxel-based morphometry: Gray matter decline in normal aging. *NeuroImage*, *60*(2), 1503–1516.

Pelletier, A., Bernard, C., Dilharreguy, B., Helmer, C., Le Goff, M., Chanraud, S., … Catheline, G. (2017). Patterns of brain atrophy associated with episodic memory and semantic fluency decline in aging. *Aging (Albany NY)*, *9*(3), 741–752.

Piras, F., Cherubini, A., Caltagirone, C., & Spalletta, G. (2011). Education mediates microstructural changes in bilateral hippocampus. *Human Brain Mapping*, *32*(2), 282–289.

Poldrack, R. (2011). Inferring mental states from neuroimaging data: From reverse inference to large-scale decoding. *Neuron*, *72*(5), 692–697.

Poldrack, R. A. (2006). Can cognitive processes be inferred from neuroimaging data. *Trends in Cognitive Sciences*, *10*(2), 59–63.

Pollitt, R. A., Kaufman, J. S., Rose, K. M., Diez-Roux, A. V., Zeng, D., & Heiss, G. (2008). Cumulative life course and adult socioeconomic status and markers of inflammation in adulthood. *Journal of Epidemiology and Community Health*, *62*(6), 484–491.

Preisig, M., Waeber, G., Vollenweider, P., Bovet, P., Rothen, S., Vandeleur, C., … Muglia, P. (2009). The PsyCoLaus study: Methodology and characteristics of the sample of a population-based survey on psychiatric disorders and their association with genetic and cardiovascular risk factors. *BMC Psychiatry*, *9*(1), 9.

R. T. Staff, Murray, A. D., Ahearn, T. S., Mustafa, N., Fox, H. C., & Whalley, L. J. (2012). Childhood socioeconomic status and adult brain size: Childhood socioeconomic status influences adult hippocampal size. *Annals of Neurology*, *71*(5), 653–660.

Raizada, R. D. S., & Kishiyama, M. M. (2010). Effects of socioeconomic status on brain development, and how cognitive neuroscience may contribute to leveling the playing field. *Frontiers in Human Neuroscience*, *4*, 3.

Raphael, D. (2011). Poverty in childhood and adverse health outcomes in adulthood. *Maturitas*, *69*(1), 22–26.

Reiss, F. (2013). Socioeconomic inequalities and mental health problems in children and adolescents: A systematic review. *Social Science & Medicine*, *90*, 24–31.

Resende, E. D. P. F., Guerra, J. J. L., & Miller, B. L. (2019). Health and socioeconomic inequities as contributors to brain health. *JAMA Neurology*, *76*(6), 633–634. Retrieved from https://jamanetwork.com/journals/jamaneurology/fullarticle/2729093

Rzezak, P., Squarzoni, P., Duran, F. L., Alves, T. D. T. F., Tamashiro-Duran, J., Bottino, C. M., … Busatto, G. F. (2015). Relationship between brain age-related reduction in gray matter and educational attainment. *PLoS One*, *10*(10), e0140945. https://doi.org/10.1371/journal.pone.0140945

Salthouse, T. A. (2009). When does age-related cognitive decline begin? *Neurobiology of Aging*, *30*(4), 507.

Sarsour, K., Sheridan, M., Jutte, D., Nuru-Jeter, A., Hinshaw, S., & Boyce, W. T. (2011). Family socioeconomic status and child executive functions: The roles of language, home environment, and single parenthood. *Journal of the International Neuropsychological Society*, *17*(1), 120–132. Retrieved from https://www.cambridge.org/core/journals/journal-of-the-international-neuropsychological-society/article/family-socioeconomic-status-and-child-executive-functions-the-roles-of-language-home-environment-and-single-parenthood/3F1BDC66DE1F7E7D87284DDD8EF18AC5

Schmierer, K., Scaravilli, F., Altmann, D. R., Barker, G. J., & Miller, D. H. (2004). Magnetization transfer ratio and myelin in postmortem multiple sclerosis brain. *Annals of Neurology*, *56*(3), 407–415.

Seidler, R., Erdeniz, B., Koppelmans, V., Hirsiger, S., Mérillat, S., & Jäncke, L. (2015). Associations between age, motor function, and resting state sensorimotor network connectivity in healthy older adults. *NeuroImage*, *108*, 47–59.

Shavers, V. L. (2007). Measurement of socioeconomic status in health disparities research. *Journal of the National Medical Association*, *99*(9), 1013–1023.

Smith, K. S., Tindell, A. J., Aldridge, J. W., & Berridge, K. C. (2009). Ventral pallidum roles in reward and motivation. *Behavioural Brain Research*, *196*(2), 155–167.

Smith, S. M., & Nichols, T. E. (2009). Threshold-free cluster enhancement: Addressing problems of smoothing, threshold dependence and localisation in cluster inference. *NeuroImage*, *44*(1), 83–98.

Steptoe, A., & Zaninotto, P. (2020). Lower socioeconomic status and the acceleration of aging: An outcome-wide analysis. *Proceedings of the National Academy of Sciences*, *117*(26), 14911–14917.

Stringhini, S., Batty, G. D., Bovet, P., Shipley, M. J., Marmot, M. G., Kumari, M., … Kivimäki, M. (2013). Association of lifecourse socioeconomic status with chronic inflammation and type 2 diabetes risk: The Whitehall II prospective cohort study. *PLoS Medicine*, *10*(7), e1001479.

Stringhini, S., Carmeli, C., Jokela, M., Avendaño, M., Muennig, P., Guida, F., … Zins, M. (2017). Socioeconomic status and the 25 × 25 risk factors as determinants of premature mortality: A multicohort study and meta-analysis of 1.7 million men and women. *The Lancet*, *389*(10075), 1229–1237.

Stumm, S. V., Smith-Woolley, E., Ayorech, Z., McMillan, A., Rimfeld, K., Dale, P. S., & Plomin, R. (2020). Predicting educational achievement from genomic measures and socioeconomic status. *Developmental Science*, *23*(3), e12925.

Tabelow, K., Balteau, E., Ashburner, J., Callaghan, M. F., Draganski, B., Helms, G., … Mohammadi, S. (2019). hMRI - A toolbox for quantitative MRI in neuroscience and clinical research. *NeuroImage*, *194*, 191–210.

Taubert, M., Roggenhofer, E., Melie-Garcia, L., Muller, S., Lehmann, N., Preisig, M., … Draganski, B. (2020). Converging patterns of aging-associated brain volume loss and tissue microstructure differences. *Neurobiology of Aging*, *88*, 108–118.

Tax, C. M., Grussu, F., Kaden, E., Ning, L., Rudrapatna, U., John Evans, C., … Veraart, J. (2019). Cross-scanner and cross-protocol diffusion MRI data harmonisation: A benchmark database and evaluation of algorithms. *NeuroImage*, *195*, 285–299.

Thompson, J. J., Blair, M. R., & Henrey, A. J. (2014). Over the hill at 24: Persistent age-related cognitive-motor decline in reaction times in an ecologically valid video game task begins in early adulthood. *PLoS One*, *9*(4), e94215.

Tottenham, N., & Sheridan, M. A. (2009). A review of adversity, the amygdala and the hippocampus: A consideration of developmental timing. *Frontiers in Human Neuroscience*, *3*, 68.

Tribble, R., & Kim, P. (2019). Intergenerational transmission of poverty: How low socioeconomic status impacts the neurobiology of two generations. In A. W. Harrist & B. C. Gardner (Eds.), *Biobehavioral markers in risk and resilience research, emerging issues in family and individual resilience* (pp. 49–67). Cham, Switzerland: Springer International Publishing, Cham.

Trofimova, O., Loued-Khenissi, L., DiDomenicantonio, G., Lutti, A., Kliegel, M., Stringhini, S., … Draganski, B. (2021). Brain tissue properties link cardio-vascular risk factors, mood and cognitive performance in the CoLaus|PsyCoLaus epidemiological cohort. *Neurobiology of Aging*, *102*, 50–63.

United Nations Economic Commission for Europe, Guidelines on producing leading, composite and sentiment indicators-draft, 2018.

Ursache, A., & Noble, K. G. (2016). Socioeconomic status, white matter, and executive function in children. *Brain and Behavior*, *6*(10), e00531.

van den Heuvel, M. P., & Hulshoff Pol, H. E. (2010). Exploring the brain network: A review on resting-state fMRI functional connectivity. *European Neuropsychopharmacology*, *20*(8), 519–534.

Voss, M. W., Nagamatsu, L. S., Liu-Ambrose, T., & Kramer, A. F. (2011). Exercise, brain, and cognition across the life span. *Journal of Applied Physiology*, *111*(5), 1505–1513.

Weiskopf, N., Mohammadi, S., Lutti, A., & Callaghan, M. F. (2015). Advances in MRI-based computational neuroanatomy: From morphometry to in-vivo histology. *Current Opinion in Neurology*, *28*(4), 313–322.

Weiskopf, N., Suckling, J., Williams, G., Correia, M. M., Inkster, B., Tait, R., … Lutti, A. (2013). Quantitative multi-parameter mapping of R1, PD*, MT, and R2* at 3T: A multi-center validation. *Frontiers in Neuroscience*, *7*, 95.

West, K. L., Kelm, N. D., Carson, R. P., Gochberg, D. F., Ess, K. C., & Does, M. D. (2018). Myelin volume fraction imaging with MRI. *NeuroImage*, *182*, 511–521.

Winkleby, M. A., Jatulis, D. E., Frank, E., & Fortmann, S. P. (1992). Socioeconomic status and health: How education, income, and occupation contribute to risk factors for cardiovascular disease. *American Journal of Public Health*, *82*(6), 816–820.

Wolff, S. D., & Balaban, R. S. (1994). Magnetization transfer imaging: Practical aspects and clinical applications. *Radiology*, *192*(3), 593–599.

Wong, C., & Gallate, J. (2012). The function of the anterior temporal lobe: A review of the empirical evidence. *Brain Research*, *1449*, 94–116.

Wozniak, J. R., & Lim, K. O. (2006). Advances in white matter imaging: A review of in vivo magnetic resonance methodologies and their applicability to the study of development and aging. *Neuroscience & Biobehavioral Reviews*, *30*(6), 762–774.

Yaple, Z. A., & Yu, R. (2020). Functional and structural brain correlates of socioeconomic status. *Cerebral Cortex*, *30*(1), 181–196.

Ziegler, G., Moutoussis, M., Hauser, T. U., Fearon, P., Bullmore, E. T., Goodyer, I. M., … Dolan, R. J. (2019). Childhood socio-economic disadvantage predicts reduced myelin growth across adolescence and young adulthood. *Human Brain Mapping*, *41*(12), 3392–3402.

**How to cite this article:** Loued-Khenissi, L., Trofimova, O., Vollenweider, P., Marques-Vidal, P., Preisig, M., Lutti, A., Kliegel, M., Sandi, C., Kherif, F., Stringhini, S., & Draganski, B. (2022). Signatures of life course socioeconomic conditions in brain anatomy. *Human Brain Mapping*, 1–25. https://doi.org/10.1002/hbm.25807

## APPENDIX A

### COHORT DESCRIPTION (Tables A1, A2, A3)

The CoLaus cohort is a representative sample of the Lausanne population (Firmann et al., 2008). However, the cohort investigated herein represents a subset of the CoLaus cohort, namely individuals who participated in the PsyColaus substudy; and who further participated in the neuroimaging study (BrainLaus). To date, the CoLaus study includes three timepoints: Baseline, Timepoint 1 and Timepoint 2. Neuroimaging data was collected at Timepoint 2.To determine if the BrainLaus cohort remained a representative cohort, we examined somatic variables in the CoLaus cohort (excluding BrainLaus participants) against the BrainLaus Cohort, finding significant differences with an effect size exceeding a Cohen's *d* of 0.2 only for age. We performed chi-square tests on categorical variables; and two sample *t*-tests on continuous ones. Below is a list of the variables compared between the two cohorts (code available at https://github.com/LLouedKhen/CoLausBrainLausComparison).

We determined whether the BrainLaus sample differed from the initial CoLaus|PsyCoLaus cohort by examining differences in a number of key variables between participants and nonparticipants of BrainLaus. (A full list of variables can be found in Table A1). There was no significant difference in sex, education level, or last known occupation distributions between the two cohorts. However, there was a significant difference in age between participants and nonparticipants of

**TABLE A1** Demographic and somatic measures at baseline

| Variable | Timepoint |
|---|---|
| Sex | Baseline |
| Age | Baseline |
| How many years lived in Switzerland | Baseline |
| Marital status (married, single, divorced, widowed) | Baseline |
| Education level (low, mid, high) | Baseline |
| Education level (years) | Baseline |
| Occupation level (low, mid, high) | Baseline |
| Number of children | Baseline |
| Swiss born (yes or no) | Baseline |
| Date of arrival in Switzerland | Baseline |
| Mini-mental state exam score (>60 years only) | Baseline |
| Minutes walked to work per day | Baseline |
| Physical activity (weekly frequency of activity >20 min, five categories) | Baseline |
| Height | Baseline |
| Weight | Baseline |
| BMI | Baseline |
| Adiponection levels | Baseline |
| Leptin levels | Baseline |
| Ferritin levels | Baseline |
| Transferrin levels | Baseline |
| c-reactive protein levels | Baseline |
| Interleukin 1 levels | Baseline |
| Interleukin 6 levels | Baseline |
| Tumor necrosis factor alpha levels | Baseline |

BrainLaus, with an average age of 59 years in participants and 63 years in nonparticipants (Cohen's $d = 0.4$). This result underlines the necessity of including age as a nuisance variable in subsequent neuroimaging analyses.

## B | COHORT CHARACTERISTICS

Below we detail the frequencies and distributions of certain demographic variables as well as individual measures of socioeconomic status present in our cohort (Figure B1).

**TABLE A2** Demographic and somatic measures at timepoint 1

| Variable | Timepoint |
|---|---|
| Age | Timepoint 1 |
| Occupation level (9 categories, ESEC) | Timepoint 1 |
| Occupation position (low, mid, high, not working) | Timepoint 1 |
| Occupation position (low, mid, high, not working, housewife) | Timepoint 1 |
| Last known occupational position (low, mid, high, not working) | Timepoint 1 |
| Social benefits (yes or no) | Timepoint 1 |
| Cardio-myopathy (yes or no) | Timepoint 1 |
| Valvular heart disease | Timepoint 1 |
| Heart failure | Timepoint 1 |
| Arrythmia | Timepoint 1 |
| Coronary artery disease | Timepoint 1 |
| Angina (yes or no) | Timepoint 1 |
| Myocardial infarction | Timepoint 1 |
| Mini-mental state exam score (>60 years only) | Timepoint 1 |
| Height | Timepoint 1 |
| Weight | Timepoint 1 |
| BMI | Timepoint 1 |
| Insulin levels | Timepoint 1 |
| Adiponection levels | Timepoint 1 |
| Leptin levels | Timepoint 1 |

## C | CHILDHOOD FINANCIAL SITUATION (Table C1)

Parental education and parental occupation were coded in the same way as own education and occupation. However, while own household income was ascertained by a direct question, its childhood equivalent was estimated by asking the following questions about the financial situation of the childhood home. Each "yes" answer was coded as 1. A cumulative score was then assigned by summing values (Table C1).

## D | IMAGE QUALITY ASSESSMENT

In order to secure reliable findings in a population study, particularly in an older age group, it is crucial to have in place a quality assessment and control protocol in place. Gross deformations, artifacts, and movement can, even with large sample sizes, significantly impact results. We implemented a four-stage QC-QA pipeline to control for outliers in the data pool (Figure D1)

1. Compute index of image quality based on movement (Castella et al., 2018). Flag data-sets >4 as 0.
2. Obtain average individual regional values (based on the Neuromorphometrics Atlas). Flag participants whose values lie beyond ±4 SD of grand mean of regional value and exclude from further processing.

**TABLE A3** Demographic and somatic measures at timepoint 2

| Variable | Timepoint |
|---|---|
| Age | Timepoint 2 (brain imaging timepoint) |
| Date of exam | Timepoint 2 (brain imaging timepoint) |
| Social benefits disability | Timepoint 2 (brain imaging timepoint) |
| Social benefits retirement | Timepoint 2 (brain imaging timepoint) |
| Employment status (currently working, yes/no) | Timepoint 2 (brain imaging timepoint) |
| Occupation position (ESEC category) | Timepoint 2 (brain imaging timepoint) |
| Hypertension (yes or no) | Timepoint 2 (brain imaging timepoint) |
| Diabetes (yes or no) | Timepoint 2 (brain imaging timepoint) |
| Cardio-myopathy (yes or no) | Timepoint 2 (brain imaging timepoint) |
| Valvular heart disease | Timepoint 2 (brain imaging timepoint) |
| Heart failure | Timepoint 2 (brain imaging timepoint) |
| Arrythmia | Timepoint 2 (brain imaging timepoint) |
| Coronary artery disease | Timepoint 2 (brain imaging timepoint) |
| Angina (yes or no) | Timepoint 2 (brain imaging timepoint) |
| Myocardial infarction | Timepoint 2 (brain imaging timepoint) |
| Alcohol consumption (yes or no) | Timepoint 2 (brain imaging timepoint) |
| Alcohol consumption, weekly rate | Timepoint 2 (brain imaging timepoint) |
| Smoking status (smoker, non-smoker, former smoker) | Timepoint 2 (brain imaging timepoint) |
| Weight | Timepoint 2 (brain imaging timepoint) |
| Height | Timepoint 2 (brain imaging timepoint) |
| BMI | Timepoint 2 (brain imaging timepoint) |
| BMI category (underweight, normal, overweight) | Timepoint 2 (brain imaging timepoint) |
| Bioimpedance measure | Timepoint 2 (brain imaging timepoint) |
| High density lipoprotein cholesterol | Timepoint 2 (brain imaging timepoint) |
| Low density lipoprotein cholesterol | Timepoint 2 (brain imaging timepoint) |
| Triglycerides level | Timepoint 2 (brain imaging timepoint) |
| Glucose level | Timepoint 2 (brain imaging timepoint) |
| c-reactive protein levels | Timepoint 2 (brain imaging timepoint) |
| Interleukin 1 levels | Timepoint 2 (brain imaging timepoint) |
| Interleukin 6 levels | Timepoint 2 (brain imaging timepoint) |
| Tumor necrosis factor alpha levels | Timepoint 2 (brain imaging timepoint) |

3. Compute difference between individual tissue masks (white matter, gray matter, CSF) and DARTEL population template. Exclude subjects whose differences exceed the grand mean of differences +2 SD (https://github.com/LLouedKhen/QCQA_MPM_DATA).
4. Of remaining subjects, identify those flagged as "0" in step 1. Visually rate these datasets (1–4, with four being excellent quality). Exclude those subjects ranking 1.

## E | COMPARISON OF WEIGHTED SES COMPOSITE SCORE VERSUS UNWEIGHTED COMPOSITE SCORE IN NEUROIMAGING RESULTS (Table E2)

SES measures used in our study are comprised of weighted composite measures of SES, with weighting factors determined by a PCA on the dataset. This procedure's net quantitative effect is to increase the amount of information within the general linear model, allowing for gradient differences in the brain to emerge. We further compared brain imaging results in unweighted versus weighted composite SES scores, to ensure that these two measures would not yield fundamentally different results (e.g., regional clusters in one and not the other).

Below, we show, as examples, results for weighted versus unweighted childhood SES results in MT maps (within gray matter masks). Weighted scores yield more higher T-thresholds but show the same spatial pattern of results (results below thresholded at $p = 0.001$, uncorrected) (Figure E1; Table E1).

For completeness, we show an example of weighted versus unweighted adult SES scores, this time in gray matter volumes. While the weighted SES measures yields slightly lower Z

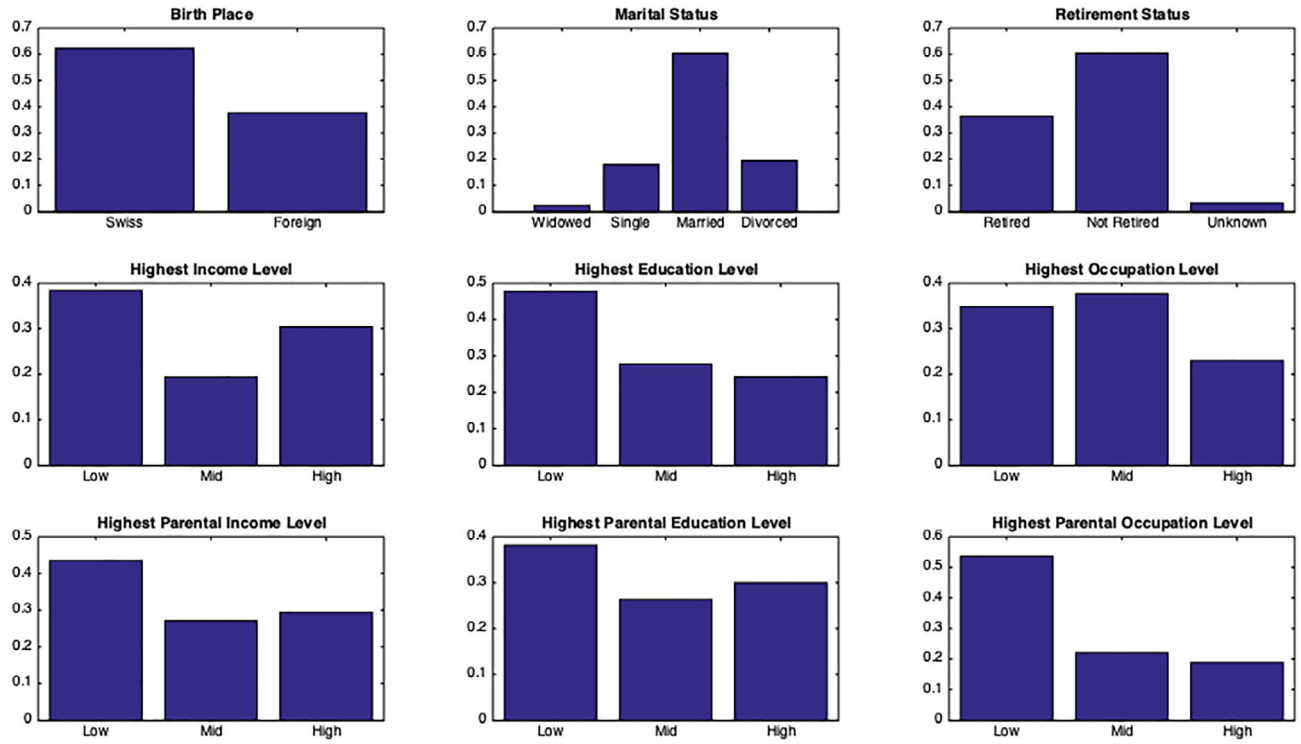


**FIGURE B1** Frequency distributions of population demographics, including marital status, birthplace, retirement status, own and parental education, income and occupation

**TABLE C1** Financial status in childhood, questionnaire

| Question | Numerical coding |
|---|---|
| Family owning a car during participant's childhood | Yes = 1 |
| Family owning a TV during participant's childhood | Yes = 1 |
| Family employing a maid during participant's childhood | Yes = 1 |
| Family owning a dish-washer during participant's childhood | Yes = 1 |
| Family owning a telephone during participant's childhood | Yes = 1 |
| Family having enough heat when cold during participant's childhood | Yes = 1 |
| Family member participating to social/cultural association during participant's | Yes = 1 |
| Family going on holidays (outside of home) during participant's childhood | Yes = 1 |
| Family owning their home during participant's childhood | Yes = 1 |

scores, the two measures nonetheless give the same clusters with only very minor variations in statistical results (Table E2).

## F | SUPPLEMENTARY AXIAL IMAGES OF MODELS 1–3, FOR MT AND GRAY MATTER (Figures F1-F6)

The images below provide additional information on the localization of results found in Models 1, 2, and 3 for MT and gray matter.

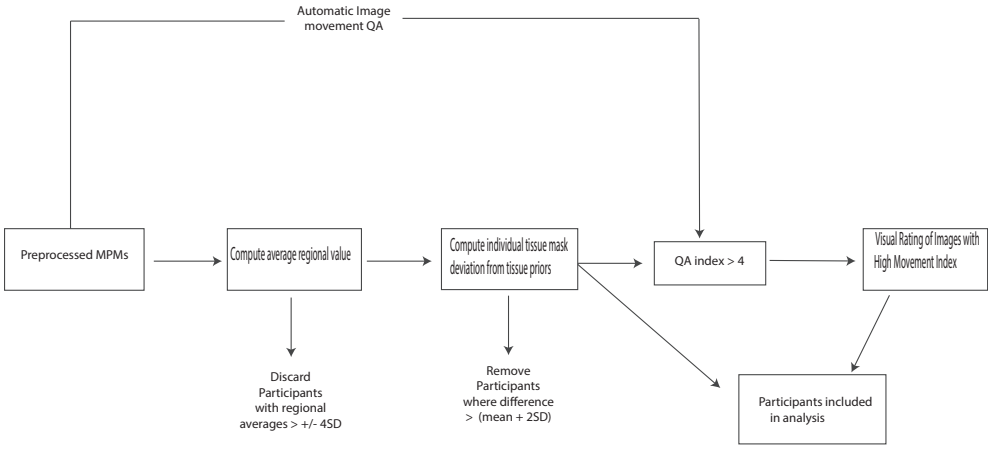


**FIGURE D1** Schematic representation of the quality control process undertaken to retain images. In a first instance, preprocessed MPMs are automatically assigned a movement index. In parallel, average values for each MPM map (PD, R2*, R1, and MT) are computed and compared to the group averages.Values across the group and within a region that fall outside 4 SD of the group mean are flagged and the associated dataset discarded. Individual tissue class masks are then compared with the canonical masks for gray matter, white matter and csf. Individual deviations greater than 2 SD from the mean are flagged and related datasets discarded. Finally, those participants remaining who have an automated movement index greater than 4 are visually inspected for excessive head movement

**TABLE E2** Gray matter volume statistics for weighted versus un-weighted childhood SES composite score

| **Gray matter volumes** | | | | | | | | | | | |
|---|---|---|---|---|---|---|---|---|---|---|---|
| Weighted childhood SES | | | | | | Unweighted childhood SES | | | | | |
| Cluster p(FWE) | Cluster *k* | Peak *Z* | Coordinates | | | Cluster p(FWE) | Cluster *k* | Peak *Z* | Coordinates | | |
| | | | *x* | *y* | *z* mm | | | | *x* | *y* | *z* mm |
| 0.002 | 150 | 5.12 | −6 | −54 | 72 | 0.001 | 235 | 5.45 | −6 | −54 | 72 |
| 0.01 | 54 | 4.79 | −12 | −21 | −6 | 0.019 | 25 | 5.14 | −18 | −22 | −18 |
| 0.035 | 6 | 4.66 | −18 | −24 | −18 | 0.012 | 45 | 4.71 | 15 | −50 | 75 |
| 0.045 | 1 | 4.52 | 9 | −52 | 74 | 0.025 | 16 | 4.67 | 32 | −78 | −54 |

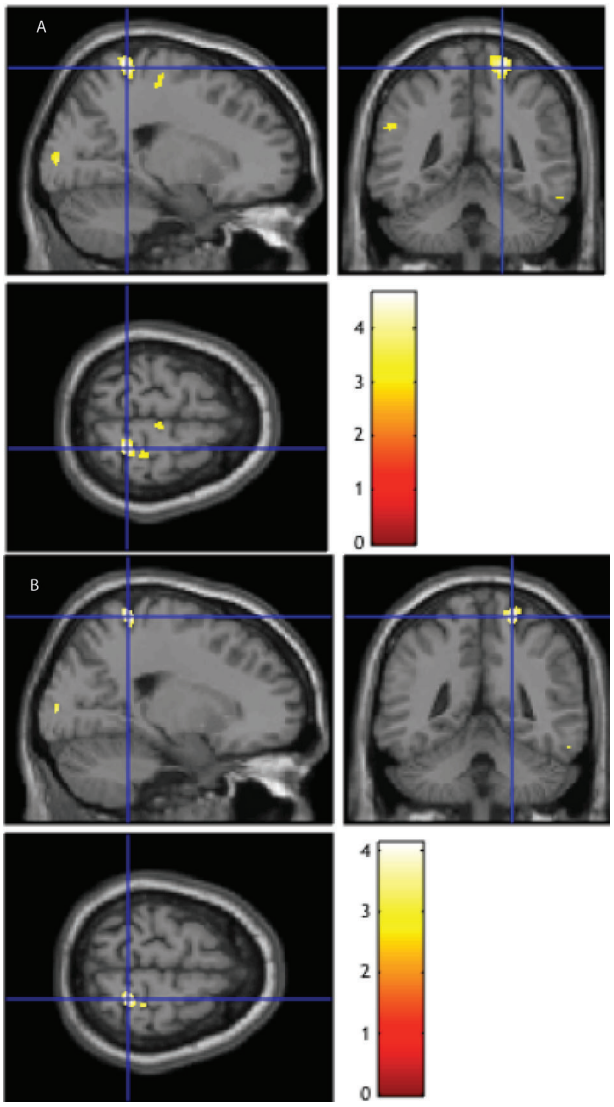


**FIGURE E1** Comparison of statistical maps for weighted vs non-weighted childhood SES associations in myelin load. (a) Statistical map of significant voxels for weighted childhood SES composite score. (b) Statistical map of significant voxels for un-weighted childhood SES composite score

**TABLE E1** MT statistics for weighted vs un-weighted childhood SES composite score

| **MT values in gray matter masks** | | | | | | | | | | |
|---|---|---|---|---|---|---|---|---|---|---|
| Weighted childhood SES | | | | | | Unweighted childhood SES | | | | | |
| Cluster p(FWE) | Cluster *k* | Peak *Z* | Coordinates | | | Cluster p(FWE) | Cluster *k* | Peak *Z* | Coordinates | | |
| | | | *x* | *y* | *z* mm | | | | *x* | *y* | *z* mm |
| 0.371 | 366 | 4.62 | 21 | −45 | 68 | 0.751 | 147 | 4.1 | 21 | −45 | 68 |
| 0.846 | 100 | 3.87 | 34 | 36 | 14 | 0.961 | 31 | 3.52 | 34 | 36 | 14 |
| 0.711 | 166 | 3.86 | 68 | −26 | −26 | 0.975 | 19 | 3.46 | −34 | 32 | 14 |
| | | 3.25 | 60 | −30 | −15 | 0.88 | 82 | 3.44 | 15 | −98 | 4 |
| 0.17 | 592 | 3.8 | −2 | −4 | −8 | 0.978 | 16 | 3.43 | −45 | −58 | 38 |
| | | 3.51 | −12 | −2 | 0 | 0.969 | 24 | 3.36 | 60 | −46 | −21 |
| 0.748 | 148 | 3.79 | 2 | −88 | 6 | 0.936 | 49 | 3.34 | −6 | −3 | −4 |
| | | 3.1 | 2 | −93 | −4 | 0.984 | 10 | 3.21 | 26 | −34 | 68 |
| 0.507 | 274 | 3.74 | 22 | −92 | 3 | 0.976 | 18 | 3.2 | 6 | −3 | −4 |
| | | 3.59 | 32 | −94 | 3 | 0.99 | 4 | 3.15 | −12 | −4 | −4 |
| | | 3.57 | 16 | −98 | 6 | 0.992 | 2 | 3.1 | 68 | −26 | −26 |
| 0.903 | 69 | 3.61 | 14 | −4 | 42 | 0.993 | 1 | 3.09 | −14 | −86 | 20 |
| 0.878 | 83 | 3.59 | 54 | 28 | −4 | | | | | | |
| 0.665 | 189 | 3.54 | 6 | −24 | 69 | | | | | | |
| | | 3.44 | 12 | −34 | 72 | | | | | | |
| 0.97 | 23 | 3.44 | −56 | −45 | 27 | | | | | | |
| 0.931 | 52 | 3.44 | −64 | −15 | −27 | | | | | | |
| 0.94 | 46 | 3.44 | 38 | −54 | 34 | | | | | | |
| 0.981 | 13 | 3.43 | −24 | −16 | 57 | | | | | | |
| 0.98 | 14 | 3.39 | −12 | −4 | 39 | | | | | | |
| 0.975 | 19 | 3.36 | 32 | 26 | 33 | | | | | | |
| 0.942 | 45 | 3.33 | 26 - | 33 | 68 | | | | | | |
| 0.973 | 21 | 3.33 | 60 | −46 | −21 | | | | | | |
| 0.949 | 40 | 3.33 | 21 | −22 | 56 | | | | | | |
| 0.979 | 15 | 3.3 | −57 | −50 | −4 | | | | | | |
| 0.985 | 9 | 3.28 | 51 | −76 | −2 | | | | | | |
| 0.883 | 80 | 3.26 | −28 | −30 | 60 | | | | | | |
| 0.984 | 10 | 3.23 | 30 | −15 | 63 | | | | | | |
| 0.979 | 15 | 3.22 | −12 | −36 | 72 | | | | | | |
| 0.991 | 3 | 3.21 | 58 | 48 | 0 | | | | | | |
| 0.984 | 10 | 3.18 | −2 | −90 | 26 | | | | | | |
| 0.99 | 4 | 3.16 | −34 | 33 | 15 | | | | | | |
| 0.982 | 12 | 3.13 | −3 | −24 | 74 | | | | | | |
| 0.993 | 1 | 3.11 | 39 | 3 | −24 | | | | | | |
| 0.993 | 1 | 3.09 | 0 | −87 | 33 | | | | | | |
| 0.993 | 1 | 3.09 | −14 | −86 | 20 | | | | | | |

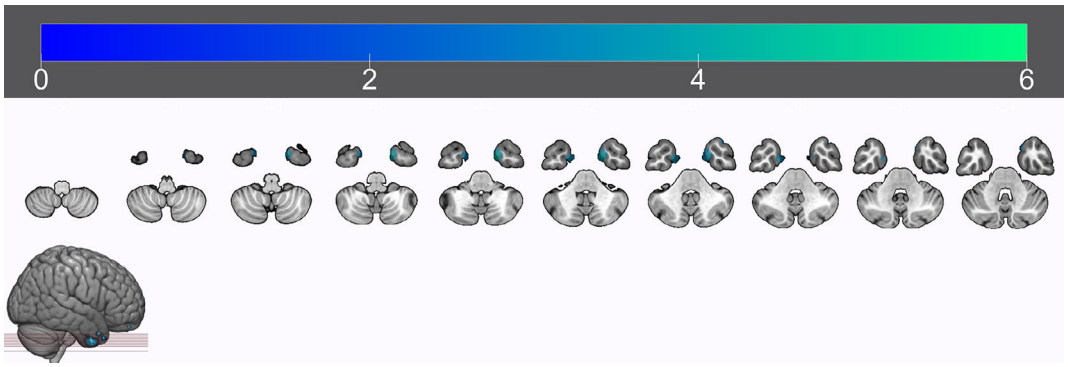


**FIGURE F1** Axial slices of results for aSES in MT for Model 1

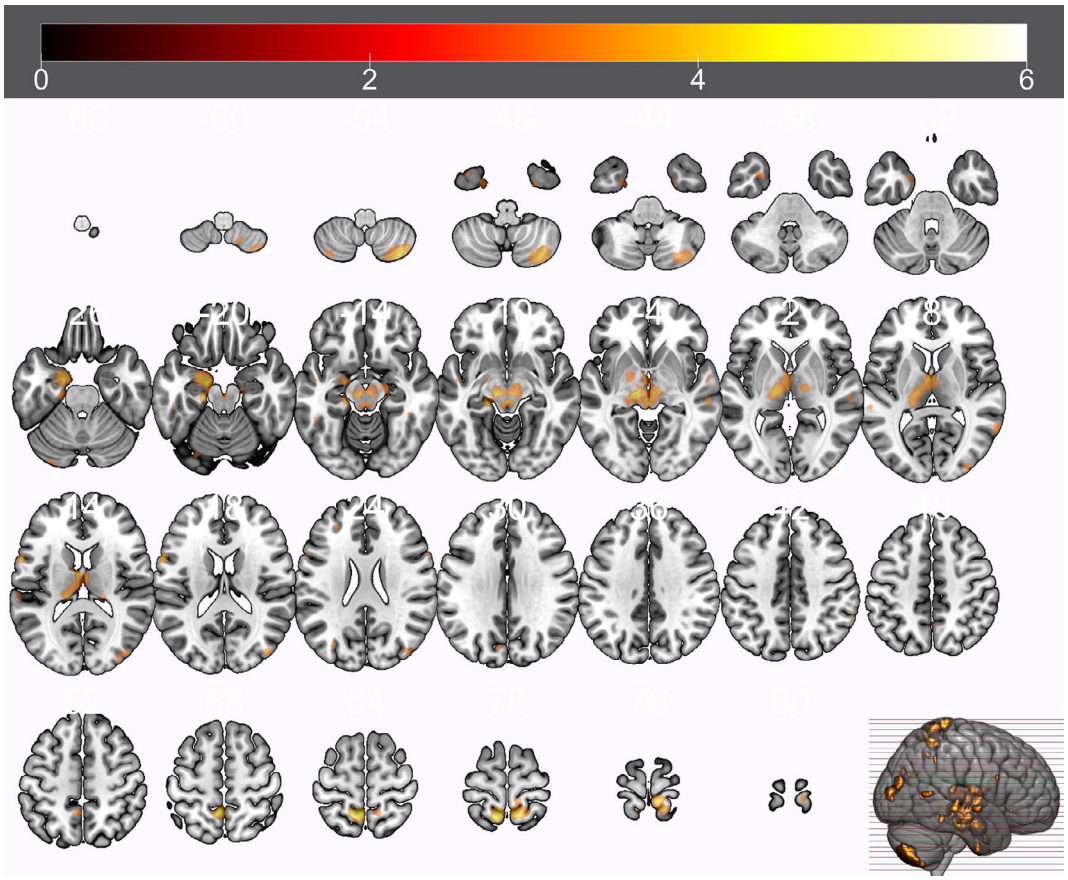


**FIGURE F2** Axial slices of results for aSES in gray matter for Model 1

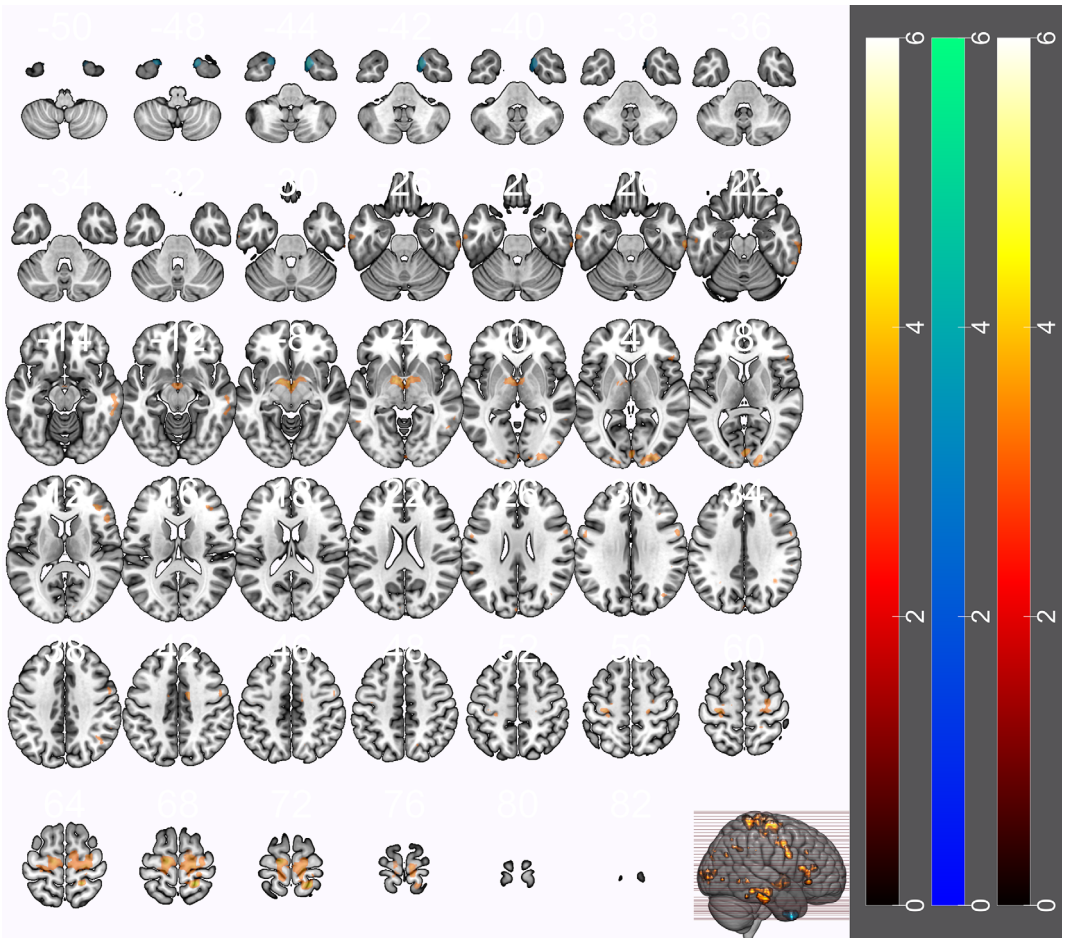


**FIGURE F3** Axial slices of results for cSES in MT for Model 2

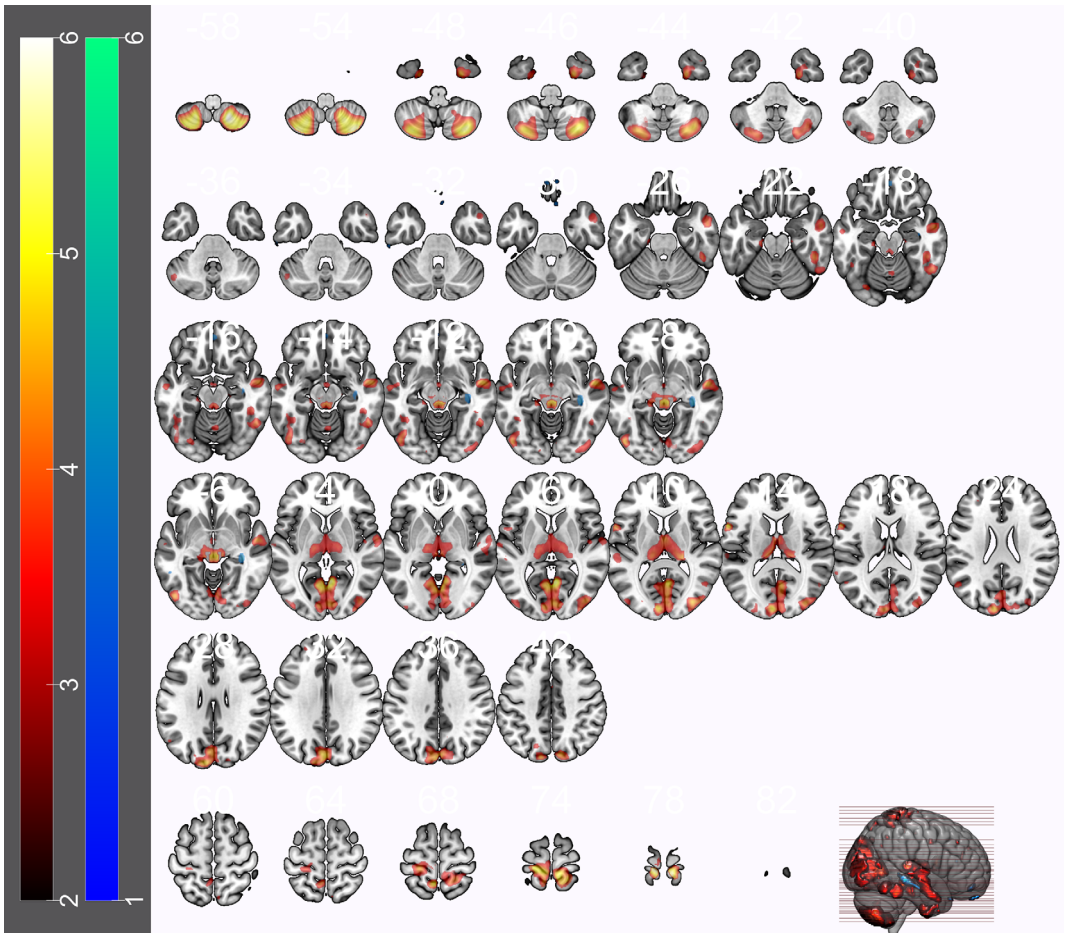

FIGURE F4 Axial slices of results for cSES in gray matter for Model 2

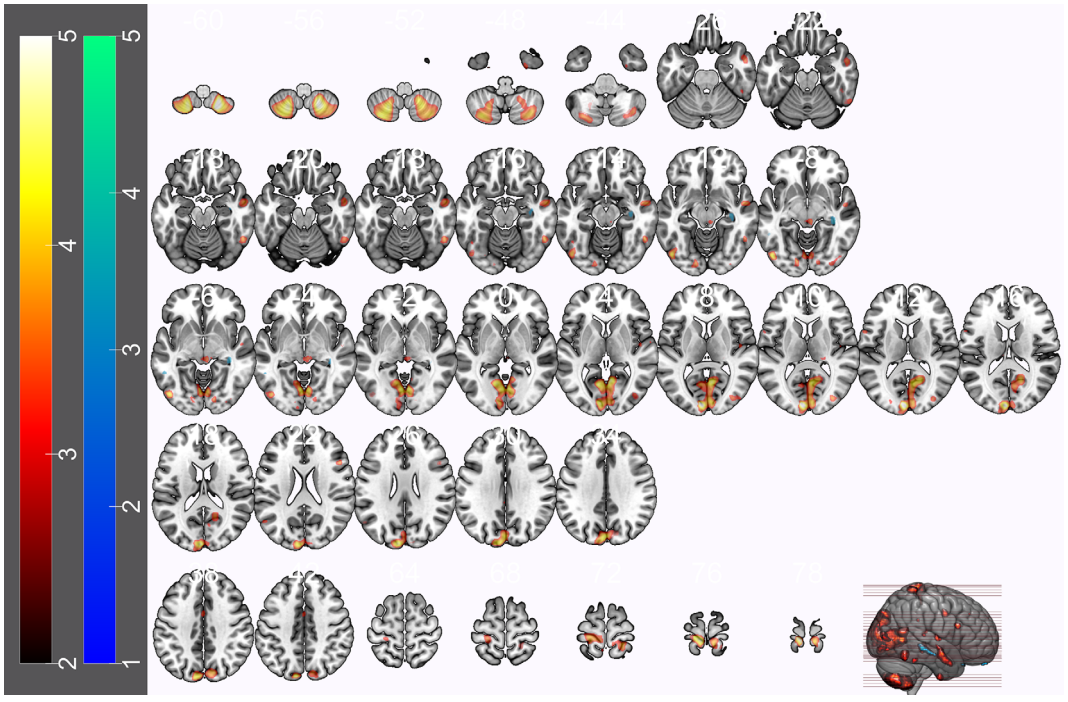

FIGURE F5 Axial slices of results for cSES in gray matter for Model 3

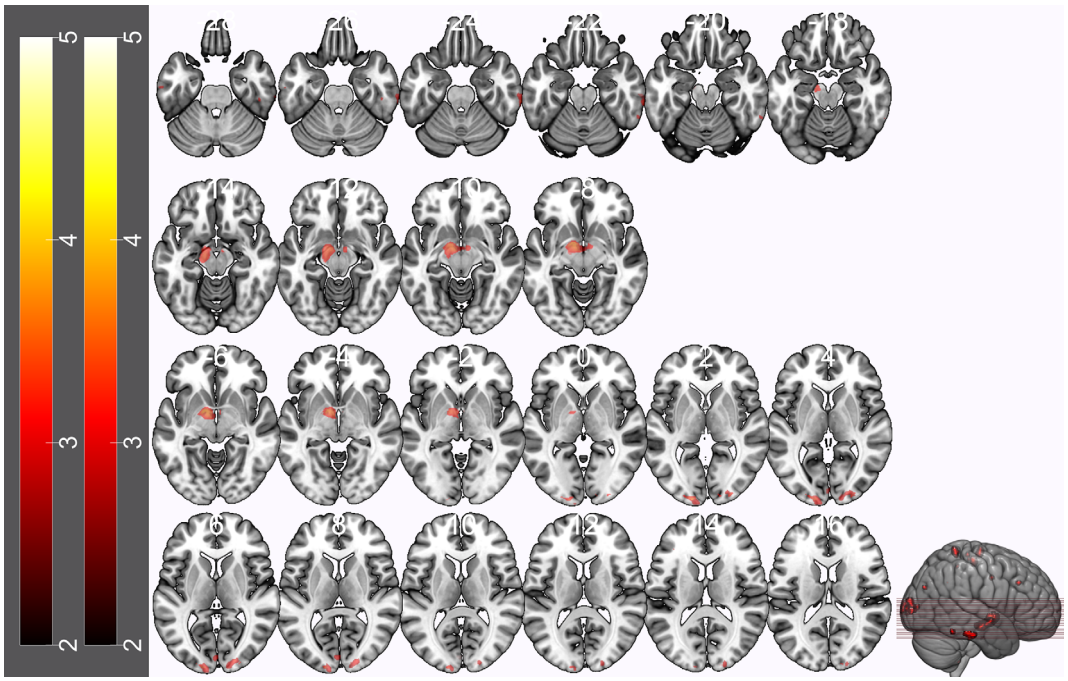


**FIGURE F6** Axial slices of results for cSES in MT for Model 3